AWI
Alfred-Wegener-Institut
für Polar- und Meeresforschung
in der Helmholtz-Gemeinschaft

ETH
Eidgenössische Technische Hochschule Zürich
Swiss Federal Institute of Technology Zurich

SIZONet 2011

Data Acquisition Report

AWI
Stefan Hendricks

ETH
Lasse Rabenstein
Jochen Lehmann-Horn
André Nuber

UAF
Hajo Eicken
Andy Mahoney

Contents

1. Overview 1
   1.1. Acknowledgements . . . 1

2. Airborne Datasets 2
   2.1. Airborne EM ice thickness . . . 2
      2.1.1. Data Processing . . . 3
      2.1.2. Flight Locations and Results . . . 3
   2.2. Aerial Photography . . . 7

3. In-Situ Data Sets 9
   3.1. Electromagnetic Induction . . . 10
      3.1.1. GEM-2 data quality . . . 11
      3.1.2. Ridge study . . . 11
      3.1.3. Profile with varying water depth . . . 12
   3.2. Surface Nuclear Magnetic Resonance . . . 20
   3.3. Electrical Resitivity Tomography . . . 23

4. Deliverables 26
   4.1. List of HEM Profiles . . . 26
   4.2. File Naming Conventions . . . 27
   4.3. Data Format . . . 27

Appendix 27

A. GEM-2 Calibration 28

Bibliography 40

1. Overview

The SIZONet project (Integrated Seasonal Ice Zone Observing NETwork) investigates the environmental, geo-political and socio-economic impact of the changing sea ice cover near the coast of the arctic ocean in Alaska. As a basic parameter, the knowledge of the thickness of the drifting sea ice as well as the landfast ice is crucial for the overall ice physics, the role of sea ice as a habitat for marine mammals and commercial operations.

As an international partner, the Alfred Wegener Institute for Polar and Marine Research (AWI) provides extensive measurements of sea ice parameters from airborne platforms and in-situ data collection. During the SIZONet 2011 field experiment, long-range sea ice thickness surveys were carried out with AWI's Polar-5 (DC-3T), a fixed-wing polar research aircraft. Polar-5 allow significant range increase compared to helicopters, which have been used in previous SIZONet field activities. In addition to the airborne measurements, a multi-instrument case study was carried out on near-shore fast ice with participation of the Swiss Federal Institute of Technology (ETH). The case study was based on data collection of different EM sensors with the prospect of enhanced EM surveying of deformed sea ice.

The purpose of this document is to give an overview of data acquisition and a summary of processing steps and data delivery format.

1.1. Acknowledgements

SIZONet is a NSF funded project (Award Nr. 0632130).

2. Airborne Datasets

Figure 2.1.: Polar-5 in Barrow during SIZONet 2011. The EM-Bird can be seen below the aircraft body.

Polar-5 is a refitted DC-3 Turbo (Basler BT-67) with science equipment for sea ice and polar meteorology research. The SIZONet 2011 field campaign was a part of the circumpolar PAM-ARCMiP (Polar Airborne Measurements and Arctic Regional Climate Model Simulation Project) campaign of Polar-5. The sea ice surveys consists of airborne EM ice thickness data, laser altimetry, aerial imagery and surface temperature from a KT19 pyrometer. During the EM data collection, Polar-5 operates in an altitude of only 200 ft, which allows for high resolution surface topography mapping at a resolution of approximately 10 cm with a Riegl Q580 airborne laser scanner. Half of the approximately 5 hour long surveys over sea ice from Barrow were used for meteorological studies in an altitude of 11500 feet and not suitable for sea ice measurements.

2.1. Airborne EM ice thickness

Electromagnetic induction sounding is a method to directly measure sea ice thickness from airborne platforms. The Alfred Wegener Institute operates a towed sensor, the so-called EM-Bird from helicopters since 2001 and from 2009 on with a fixed-wing aircraft (Polar-5).

During the ice surveys, the EM-Bird is towed at an altitude of 10-15 meters above the sea ice surface. A transmitter/receiver pair of coils operating at a frequency of 4.09 kHz is used to estimate the distance of the instrument to the ice-water interface. A laser altimeter records the height above the sea ice surface, hence ice thickness can be obtained by the difference of both distances. Since the laser altimeter is reflected at the top snow surface, the resulting thickness value always includes the thickness of the snow layer, if present.
Because of the required survey altitude and the disturbing effect of the airplane fuselage, the EM-Bird is lowered towards the surface on a 200 ft long tow cable with a winch inside the cabin. Real-time telemetry of the EM-Bird is displayed to the pilots for altitude control of the instrument. The sensor is retracted by the winch and latched to aircraft body after the completed survey.

2.1.1. Data Processing

The airborne EM data is calibrated in regular intervals of 10 minutes and by measurements over of open water along the profile. The 1D processing is based on the assumption of a homogenous halfspace with the sea water as the only conductor (el. conductivity 2400 mS/m). The thickness of deformed sea ice such as pressure ridges may be underestimated by as much as 50%, depending on the ridge geometry. For post-processing, a small window sliding-mean boxfilter is applied to the ice thickness data to reduce the effect of EM noise on the raw data.

2.1.2. Flight Locations and Results

Two flights were performed on March 30 and April 2 by the Polar-5 group. During the surveys the EM-Bird was used for sea ice thickness retrieval, an airborne laser scanner for topography mapping and a nadir looking camera for aerial photography. The motivation for the first flight was to capture the ice thickness distribution at specific locations west of Point Barrow, while the second flight aimed for a band of multiyear sea ice north-east of Barrow. The locations of the flight lines are shown in Figure 2.3.

Survey 1 (2011/03/30)

The flight track lead to positions of upward looking sonars (ULS) in the region west of Barrow as well as Hanna Shoal, a shallow site of recurring ice grounding. The sea ice thickness distribution of the EM-Bird (Figure 2.4) indicates heavy ice deformation in this region with a broad distribution and a significant amount of thicknesses above 2 meters . The high mean thickness of 2.9 meter is close to values found in multi-year ice regions. Over Hanna Shoal, thicknesses of up to 35 m were found (Figure 2.5). However, due to degradation of the signal strength with increasing ice thickness the error

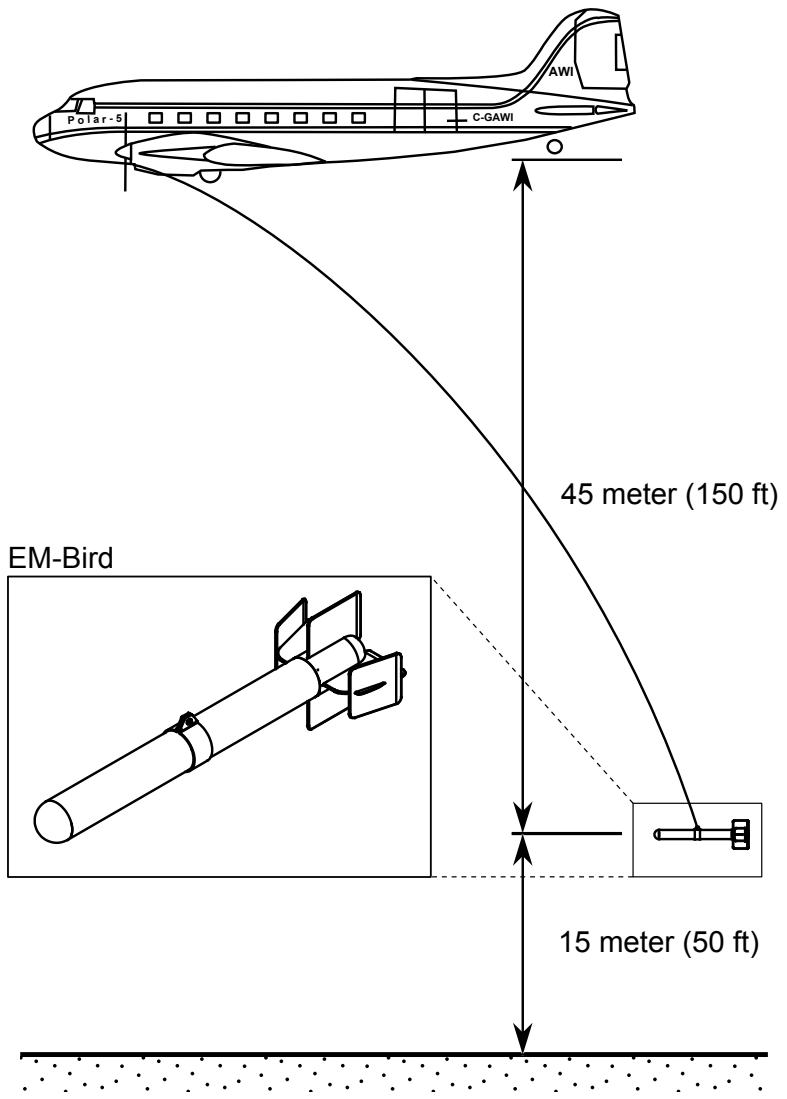

Figure 2.2.: EM-Bird in operational mode on Polar-5. The 200 ft tow cable provides power to the instrument. Real-time data transfer is realized by a wireless network.

caused by instrument noise is in the order several meters. In addition, the airborne EM method tends to underestimate maximum pressure ridge thickness by 50-80%. Simulations have shown that this effect is less pronounced for the thickest class of ridges (> 25 m). Another error source is given by the seafloor below the ridges, which is not included in the standard processing of airborne EM data. The sea floor has a lower el. conductivity than sea water and may cause a thickness bias if the sea ice would be grounded on a broad (100 m) area. The thickest ice appears in narrow peaks, for which the influence of the seafloor (at 20 m depth) can be neglected. Therefore we assume that the maximum thicknesses observed here give a reasonable representation of the thickness of deformed and grounded sea ice within an accuracy of +/- 5 meters.

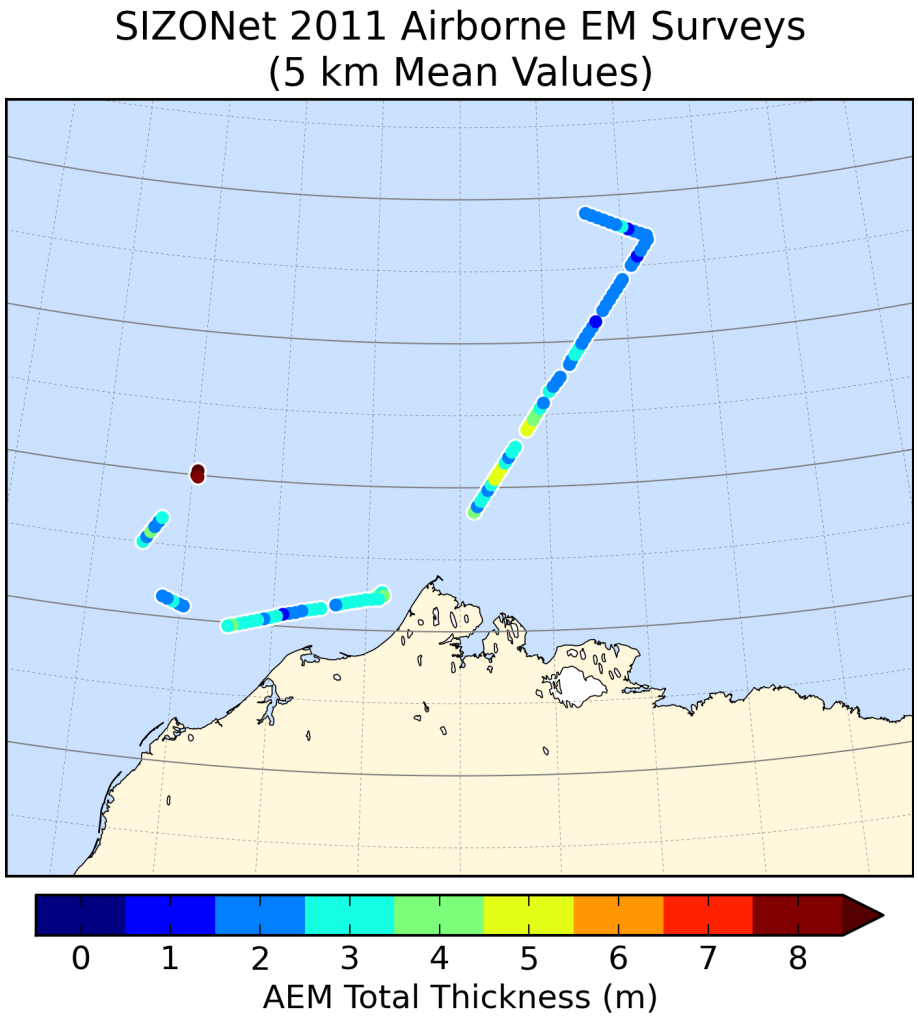

Figure 2.3.: Mean sea ice thickness averaged over 5 km sections for two flights during the SIZONet 2011 field experiment. 2011/03/30: West of Barrow, 2011/04/04 North-east of Barrow

Survey 2 (2011/04/02)

The second flight was directed towards a zone of scattered multi-year ice floes around 74°N north-east of Barrow. The sea ice thickness distribution is distinctively different from survey 1: The distribution shows a clear peak which represents the thickness of undeformed first-year sea ice. Sea ice with thicknesses larger than 2 m was observed less frequently and was mostly limited to the southern part of the profile (Figure 2.3). However, it should be noted that some section show mean thicknesses of up to 5 m for 5 km section and therefore indicate the presence of heavy ice deformation. Unfortunately, only very few multiyear ice floes were observed along the flight path. Therefore a comparison of the thickness distribution of first-year and multi-year sea ice cannot be given from this data.

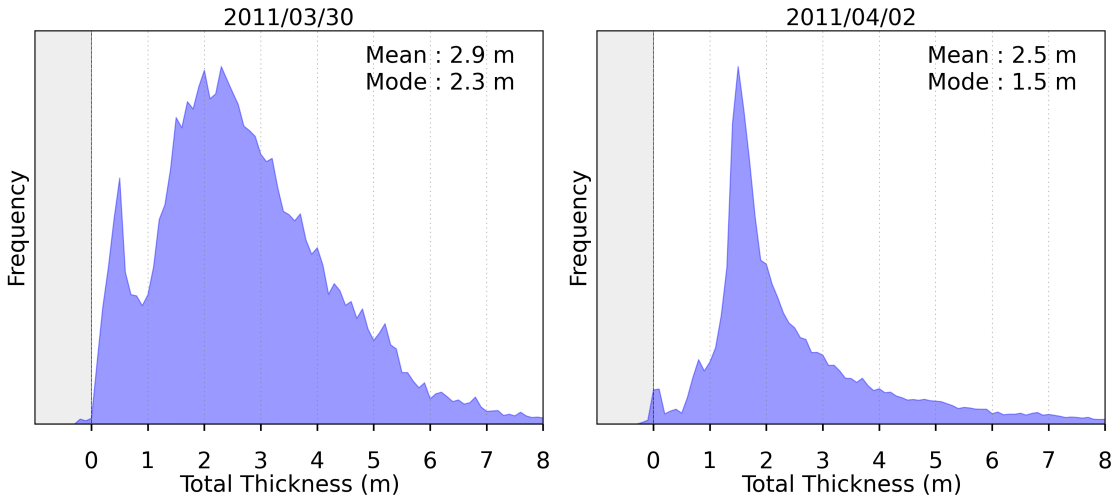

(a) (b)

Figure 2.4.: Sea ice thickness histograms from both Polar-5 surveys

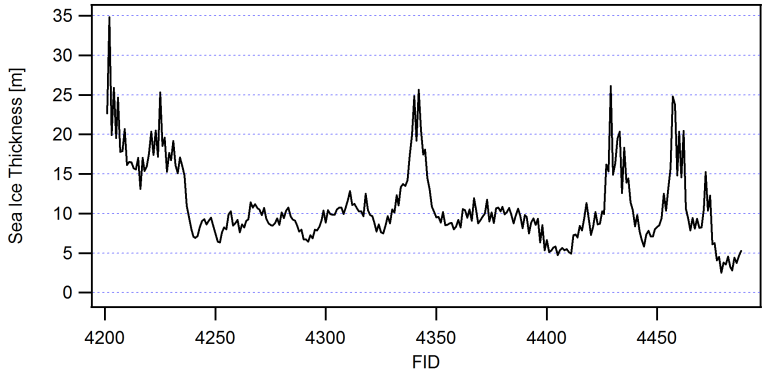

(a)

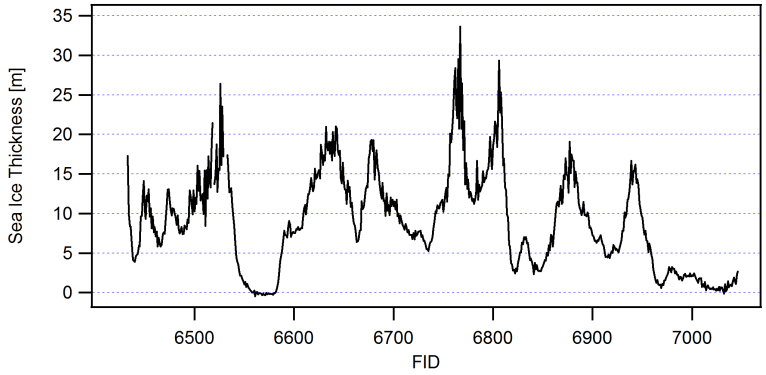

(b)

Figure 2.5.: Sea ice thickness from two overflights (perpendicular crossings) over Hanna Shoal. (FID: record number)

2.2. Aerial Photography

Nadir images have been taken from Polar-5 with an Canon EOS 1D MkIII digital camera equipped with a 14 mm wide angle lens. A photo is taken every 6 seconds which is sufficient for overlapping of successive images at an altidude of 1000 ft. During ice thickness surveys with an aircraft altitude of 200 ft, images do not overlap. In addition, the images contain the tow cable and partly the EM-Bird during the surveys.
The camera is synchronized with the GPS system of the aircraft, which allows together with the INS information a geolocation of each pixel. Data is availible during the entire survey of March 30th during low level of the sea ice survey and high level of the meteorological survey. On April 2nd, images do not exist during the EM survey but over landfast sea ice close to Barrow. Due to instabilities of the data inferface, the images do not contain GPS positions in their EXIF tags for the sea ice survey on March 30. However, the positions of each image can be calculated by the onboard GPS system of Polar-5.

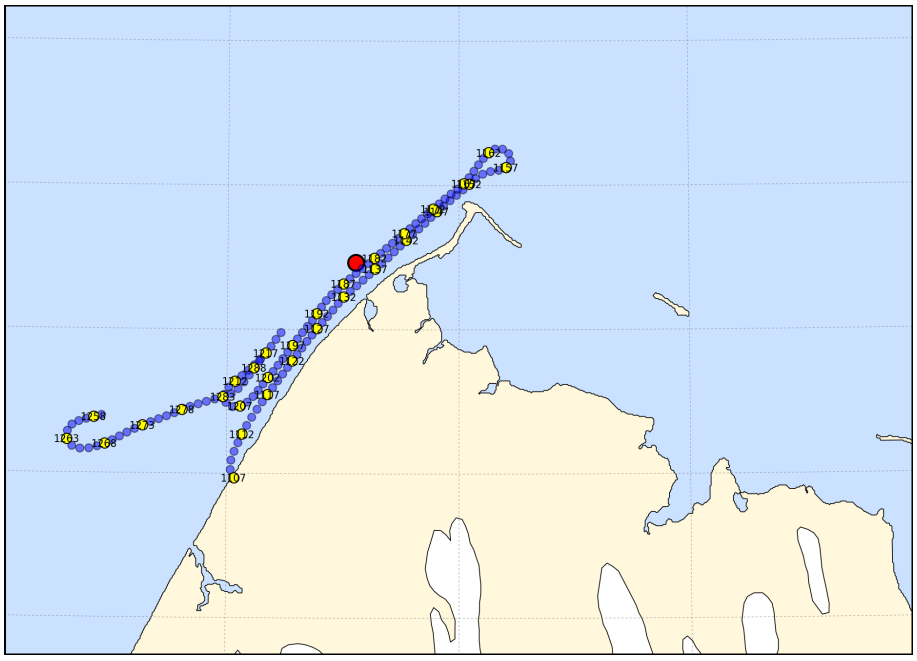

Figure 2.6.: Map of photo locations along survey over fast ice zone. The red dot marks the site of the EM multi-sensor study (not covered by any image)

Figure 2.7.: Example of image composite over Barrow landfast sea ice at the location of a whaling trail

3. In-Situ Data Sets

A selected pressure ridge in the landfast sea ice west of Barrow was the site of a multi-sensor study with several geophysical EM methods. The aim of this study was to investigate

a the feasibility of estimating water content of pressure ridges with Surface Nuclear Magnetic Resonance (SNMR) measurements

b the potential of multi-frequency EM data for an enhanced ice thickness retrieval including internal sea ice properties such as porosity or detection of ridge grounding in shallow areas

The major part of the data collection took place at one pressure ridge, which was chosen based on the linear appearance of the sail. This linearity suggested a 2D ridge geometry structure which is necessary for this case study. One side of the ridge consists of first-year level ice, while the other side showed topography features of a deformation event. The water depth was around 21 m and there was no indication that the ridge was grounded.
The data collection comprised different EM methods and other in-situ observation:

SNMR is sensitive to water in its liquid phase and therefore to the sea water filled voids in the keel of the pressure ridge

Electromagnetic induction (EM) is based on the distribution of electrical conductivity in the ridge, which can be related to porosity

Electrical Resistivity Tomography (ERT) is an additional method to get independent estimates of the electrical conductivity distribution

Steam drilling was used for ground truthing of ice thickness and for the mapping of voids in the ridge keel

Differential GPS completes the dataset with a topography model of the ridge surface

The measurements were aligned along three line with a length of 100 meter each and a spacing of 10 meter with an orientation perpendicular to the strike direction of the ridge (see Figure 3.1). The lines define a right-handed reference frame, with the origin of the coordinate system at the top of the ridge of the center line. EM data is availiable

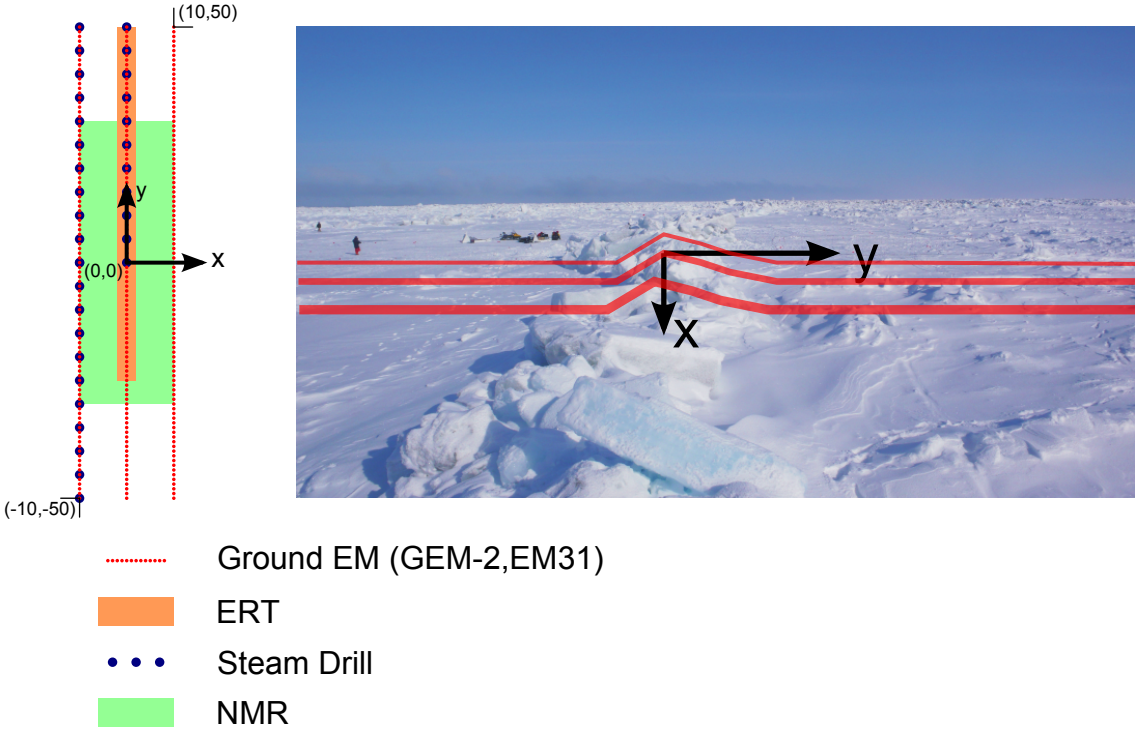

Figure 3.1.: Layout of measurements of a multi-sensor study of a pressure ridge in landfast sea ice. Three lines with an individual length of 100 m and a spacing of 20 meters were used to align data collected from EM sensors and drilling

on all lines, while drill data was obtained on one full line (x = -10) and one line (x = 0) at only on side of the ridge. ERT data is availiable on the center line. and A more detailed description of the data collected by the different methods is given in the following sections.

3.1. Electromagnetic Induction

Electromagnetic induction sounding was carried out with two sensors, a „classical" EM31 MKII and a GEM-2 rented from Geophex Ltd. The GEM-2 is multi-freqency EM instrument with programmable frequencies between 300 Hz and 96 kHz and a coil-spacing of 1.66 m. Four frequencies were used during the surveys: 330 Hz, 990 Hz, 3990 Hz and 9990 Hz compared to 9660 Hz of the EM31. The lowest frequency of 330 Hz is typically used for bathymetry mapping, while the choice of 990 Hz is based on model runs for the sounding of the lower part of pressure ridges. The higher frequencies of 3990 Hz and 9990 Hz are close to the ones used for the EM-Bird and EM31, respectively. The GEM-2 records data at 20 Hz, stacking based on time or location was implement in the post-processing depending on whether the instrument was stationary or used as a rover.

3.1.1. GEM-2 data quality

Since the GEM-2 was not used by the AWI-ETH group before in the field for sea ice applications, the instrument was tested for its thermal stability in a low temperature environment and typical EM noise. In this test, the instrument was operated undisturbed on the sea ice surface for 30 minutes. The EM noise was analyzed for the full data rate of 20 Hz and a stacked time series of 1 Hz. The results are shown in the Appendix of this report (see Figures A.1 - A.4). Amplitude and phase drift does exist in all frequencies with a comparable magnitude (> 200 ppm / 30 minutes). This is a manageable level for the higher frequencies but becomes more severe for the lower frequencies where the drift is a significant fraction of the total signal level. The lower ppm range of the lower frequencies is also more affected by noise, while at the two higher frequencies noise is almost insignificant when using the 1 Hz stacked data. Therefore all data collected in the field experiment was stacked to a 1 Hz resolution and certain location where repeatedly measured (where applicable) to monitor sensor drift.

3.1.2. Ridge study

All three lines of the ridge field site were surveyed with the GEM-2 in 1 meter steps using three measurement modes. The three modes consists of 2 horizontal coplanar (HCP) measurements (sensor aligned along-track and across-track) on the ground and a vertical-coplanar (VCP, sensor tilted by 90°) with the instrument at hip height. Differences in the two HCP modes can be used to detect small-scale 3D inhomogeneities, while the VCP mode changes the induction patterns and hence the sensitivity of the sensor for certain structures.
The results are displayed for the EM parameters (Inphase & Quadrature, Amplitude & Phase) in the Figures 3.2 - 3.7). For the HCP modes, no frequency shows any negative effect of either significant drift or instrument noise. The ridge can be clearly identified in the all three lines, while the sensitivity is reduced for the lower frequencies as expected. The GEM-2 data also matches the visual observations of deformed level ice on the one side (y = +30 – +50 m) of the main ridge.
The VCP data however seems to be of poor quality. The main features are visible, but a significant number of outliers and unjustified jumps in the EM channels prevent a useful analysis of the VCP data. The reason might be the sensitivity of the GEM-2 to small sources close to the sensor and changing orientation of the instrument during stacking. Therefore it is advised for sea ice studies to operate the GEM-2 on the ground in the absence of metal parts close to the sensor.
Figure 3.8 shows the thickness results of the EM31 ice and the drilling along the line of x = -10 m. The underestimation of the ridge thickness by the EM31 is more pronounced in areas where several voids exist. The general shape of the drill data resembles the GEM-2 data nicely, which also seems to better resolve some thickness features between 30 and 40 meters than the EM31.

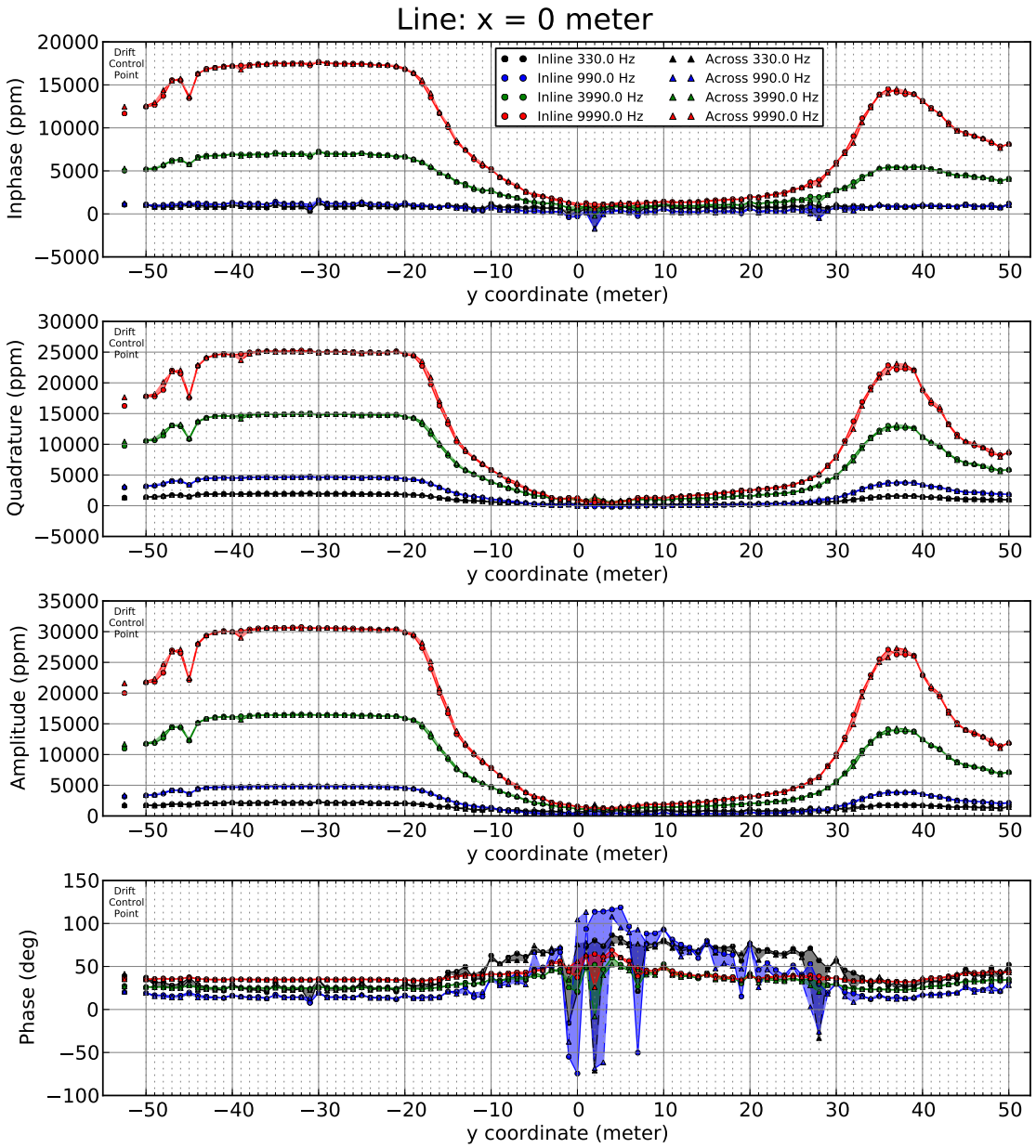

Figure 3.2.: Horizontal coplanar (HCP) multi-frequency EM data of ridge at line x = 0

3.1.3. Profile with varying water depth

The GEM-2 was also towed in a sled to retrieve multi-frequency EM data over a variety of sea ice types. The approximately 3 km long surveys started on presumably grounded sea ice very close to the shore and followed a trail leading to the ridge site. The trail crossed areas of level ice as well as ice deformation zones, which might had been grounded with increasing depth further offshore.

It was planned to use a skidoo to tow the plastic sled, however the electromagnetic noise caused the skidoo was to strong for meaningful measurements. Therefore the

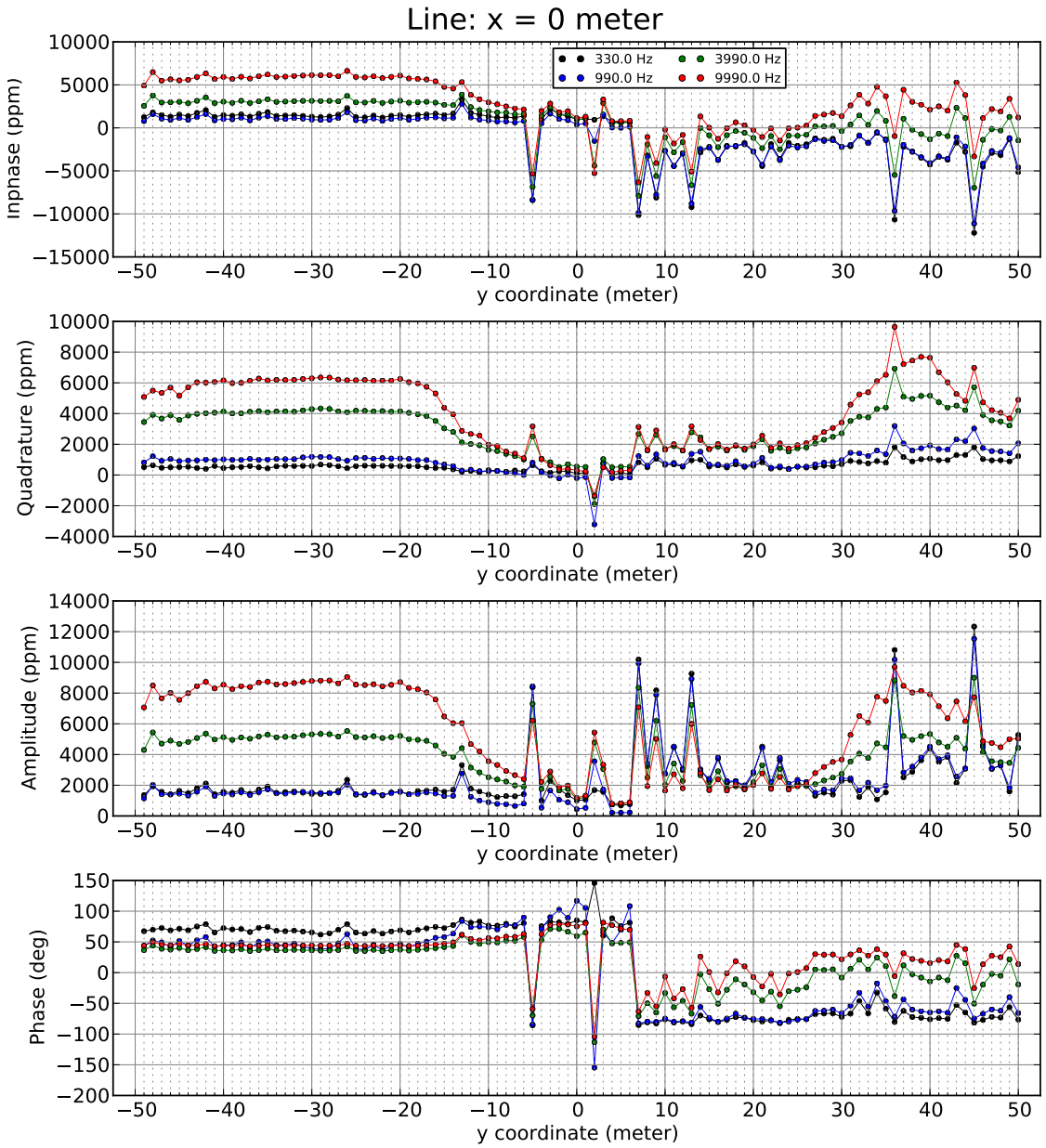

Figure 3.3.: Vertical coplanar (VCP) multi-frequency EM data of ridge at line x = 0

sled was towed manually. It was observed that movements of the bolt of the sleds coupling as well a GPS handheld device do have a measurable effect on the GEM-2. For future studies it is advised that the least amount of metal parts shall be used.
The location of the trail is shown in Figure 3.9 and the corresponding EM data in Figure 3.10.

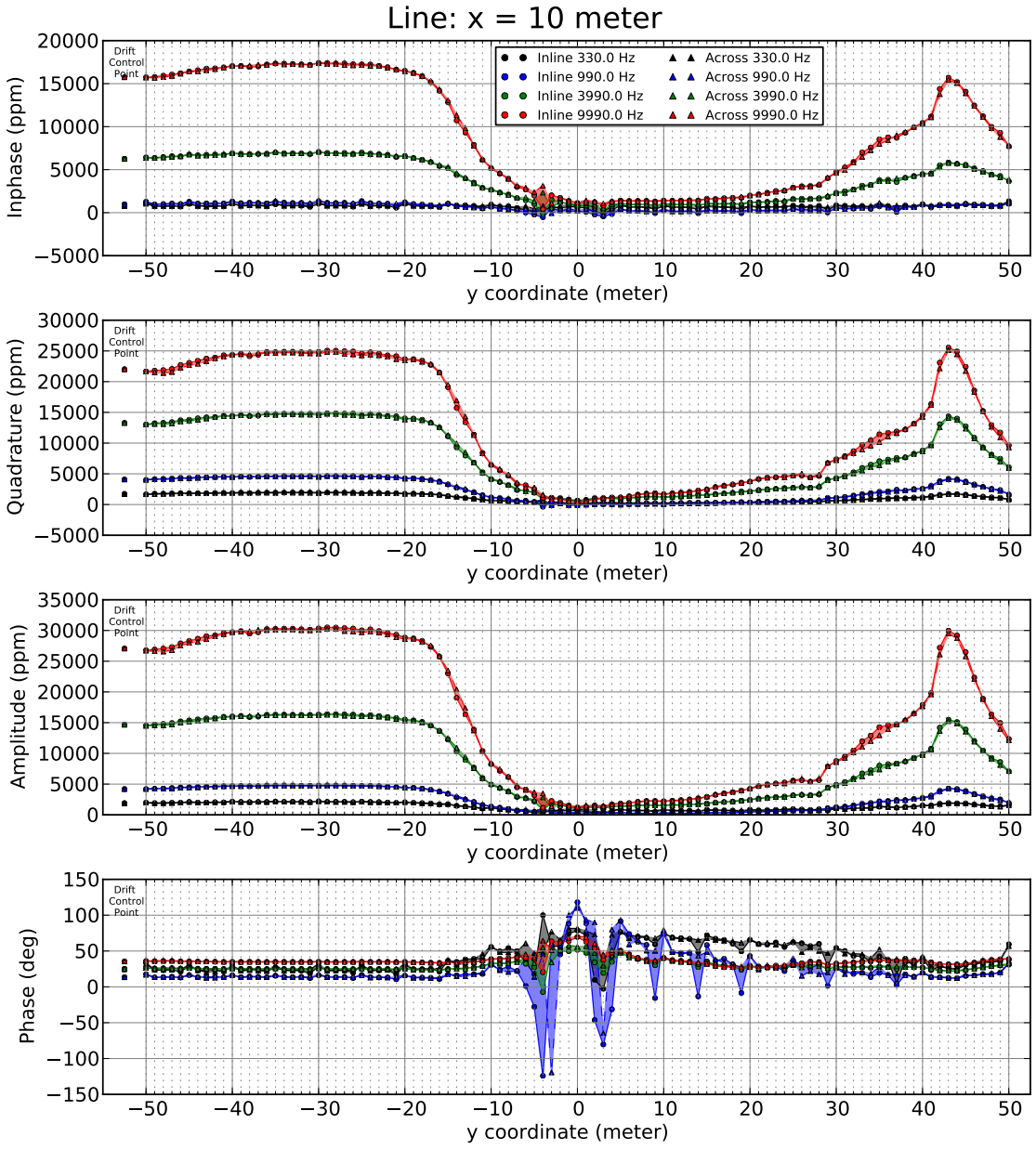

Figure 3.4.: Horizontal coplanar (HCP) multi-frequency EM data of ridge at line x = 10

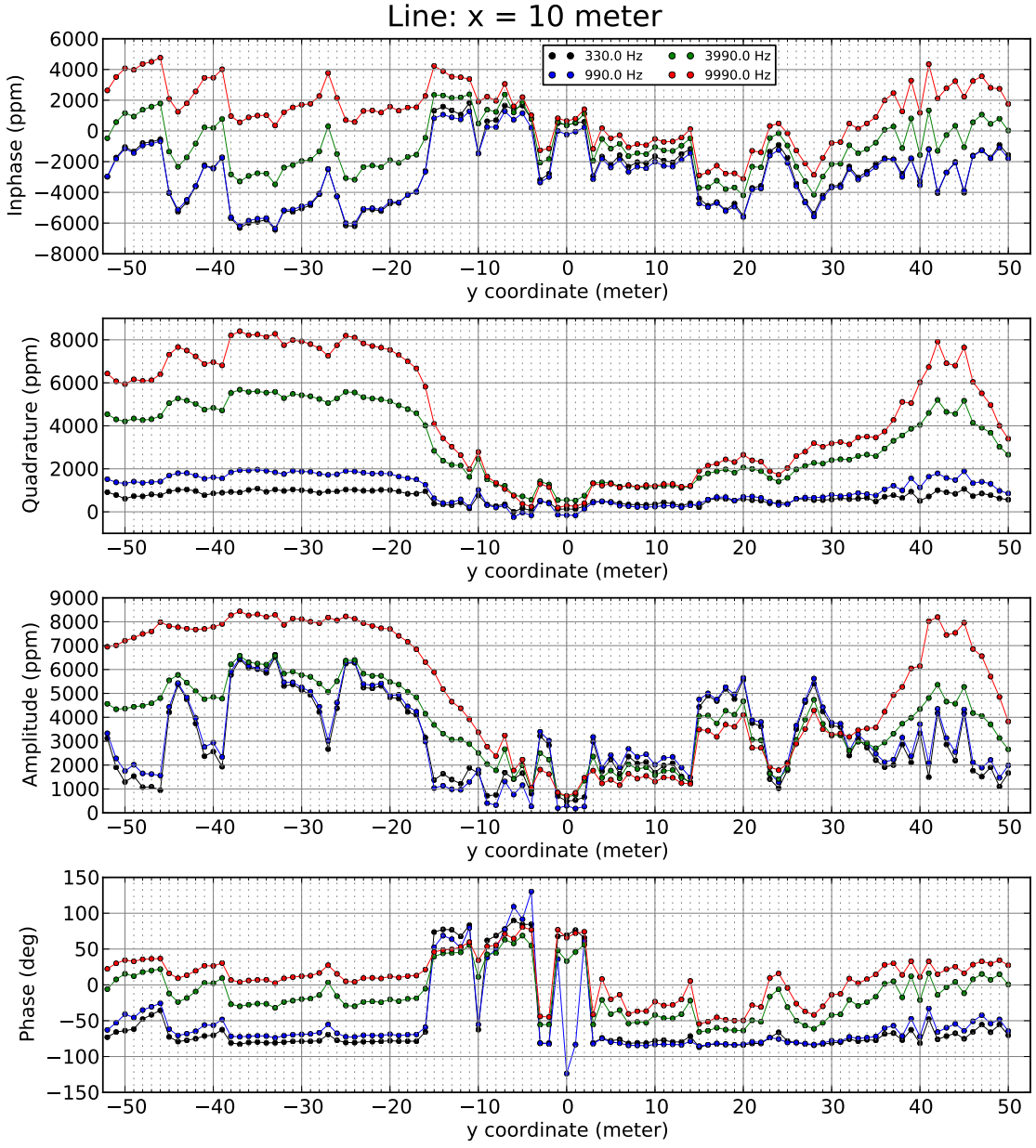

Figure 3.5.: Vertical coplanar (VCP) multi-frequency EM data of ridge at line x = 10

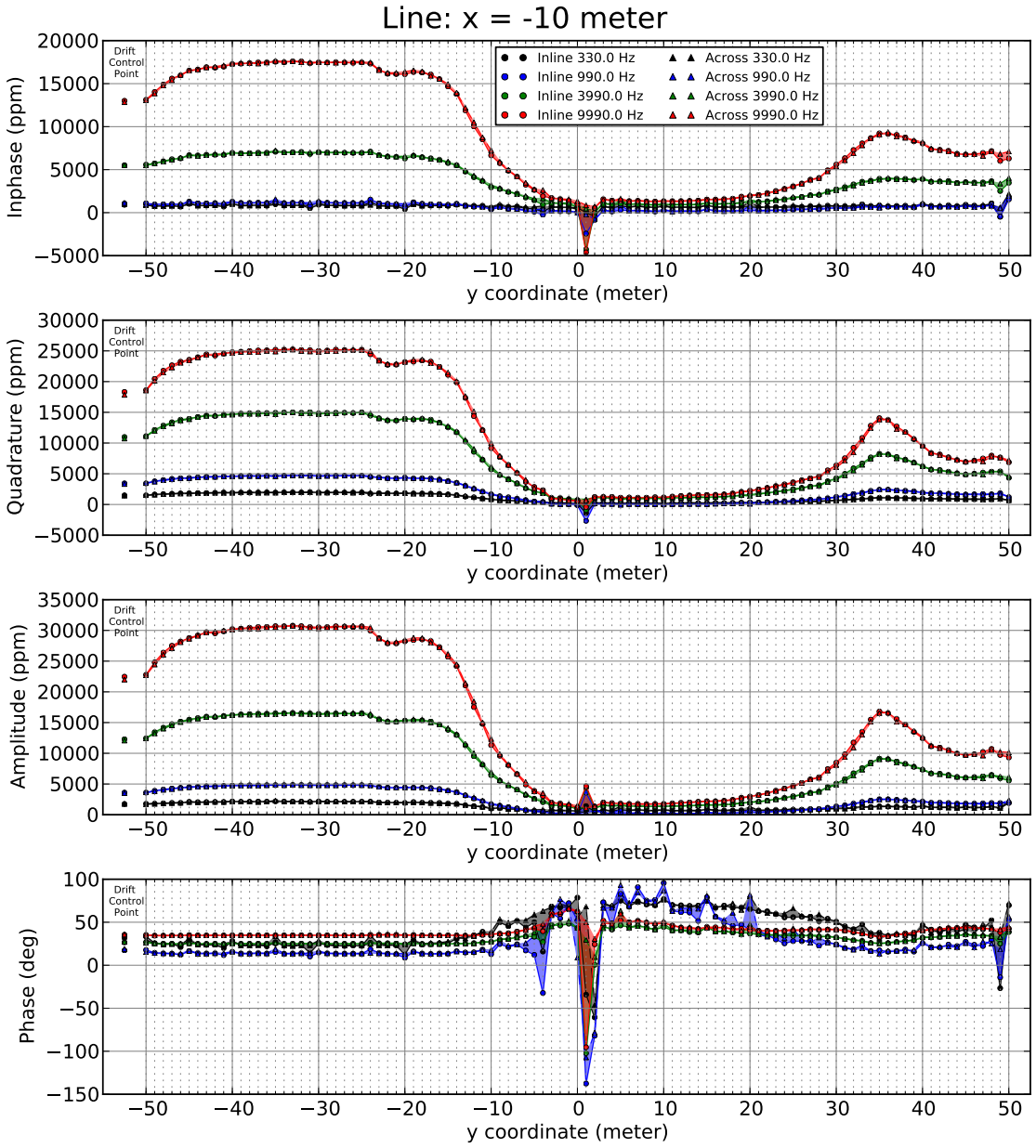

Figure 3.6.: Horizontal coplanar (HCP) multi-frequency EM data of ridge at line x = -10

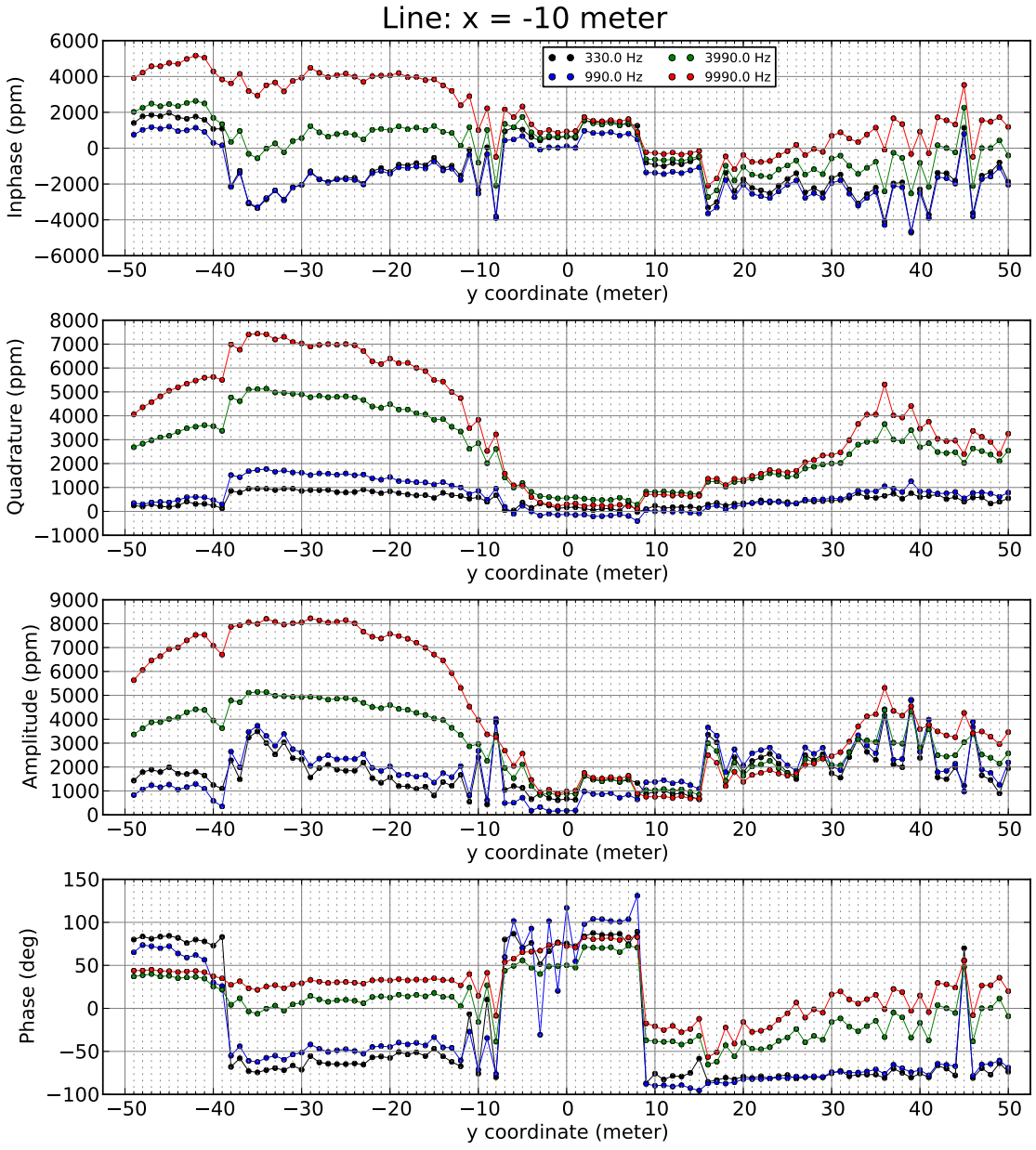

Figure 3.7.: Vertical coplanar (VCP) multi-frequency EM data of ridge at line x = -10

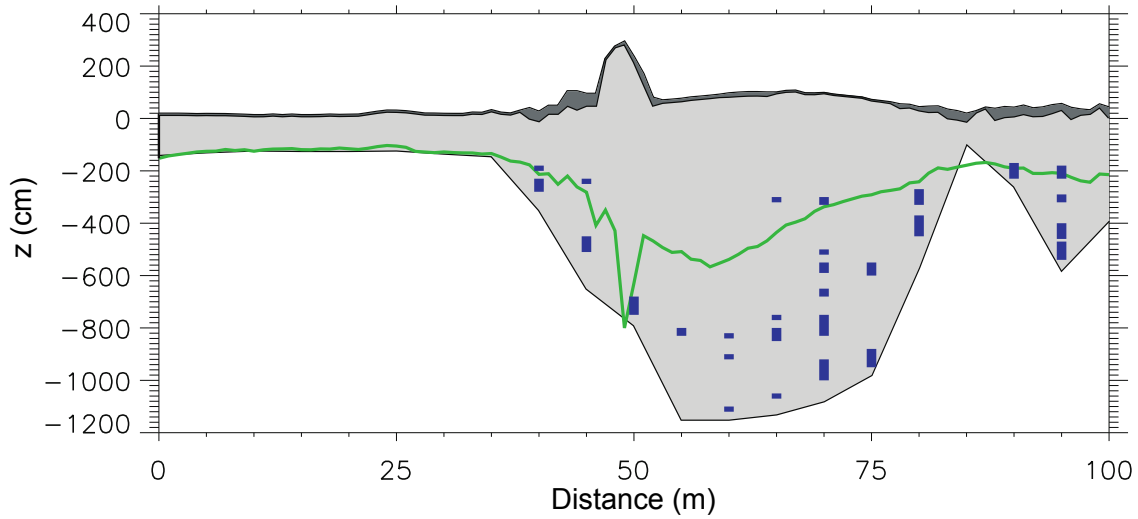

Figure 3.8.: Sea ice thickness obtained from the EM31 and steam drilling together with the locations of voids in the ridge

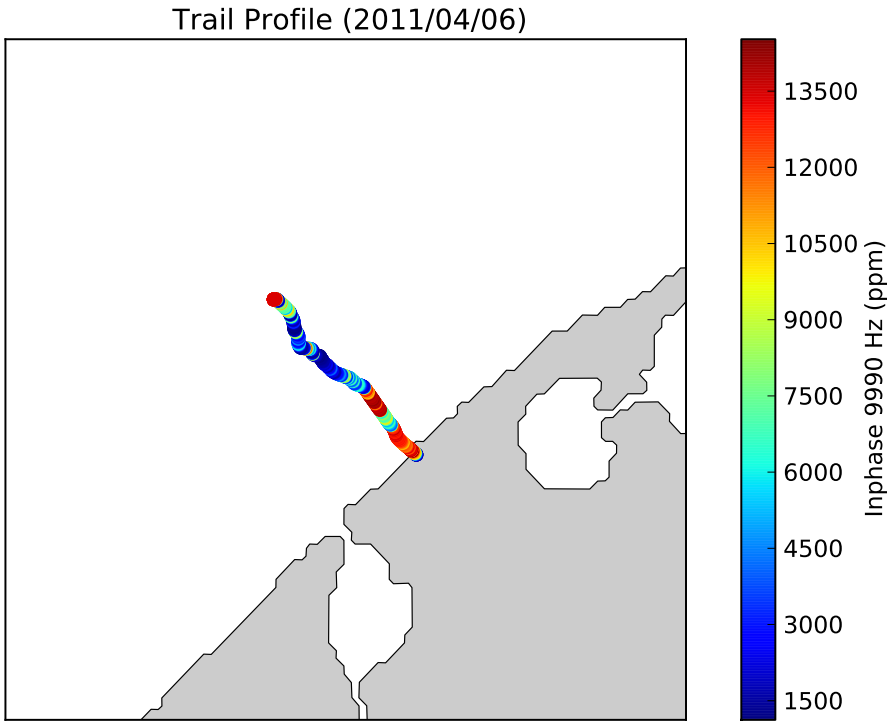

Figure 3.9.: Location of trail surveyed with GEM-2. (Color: Inphase 9.99 kHz)

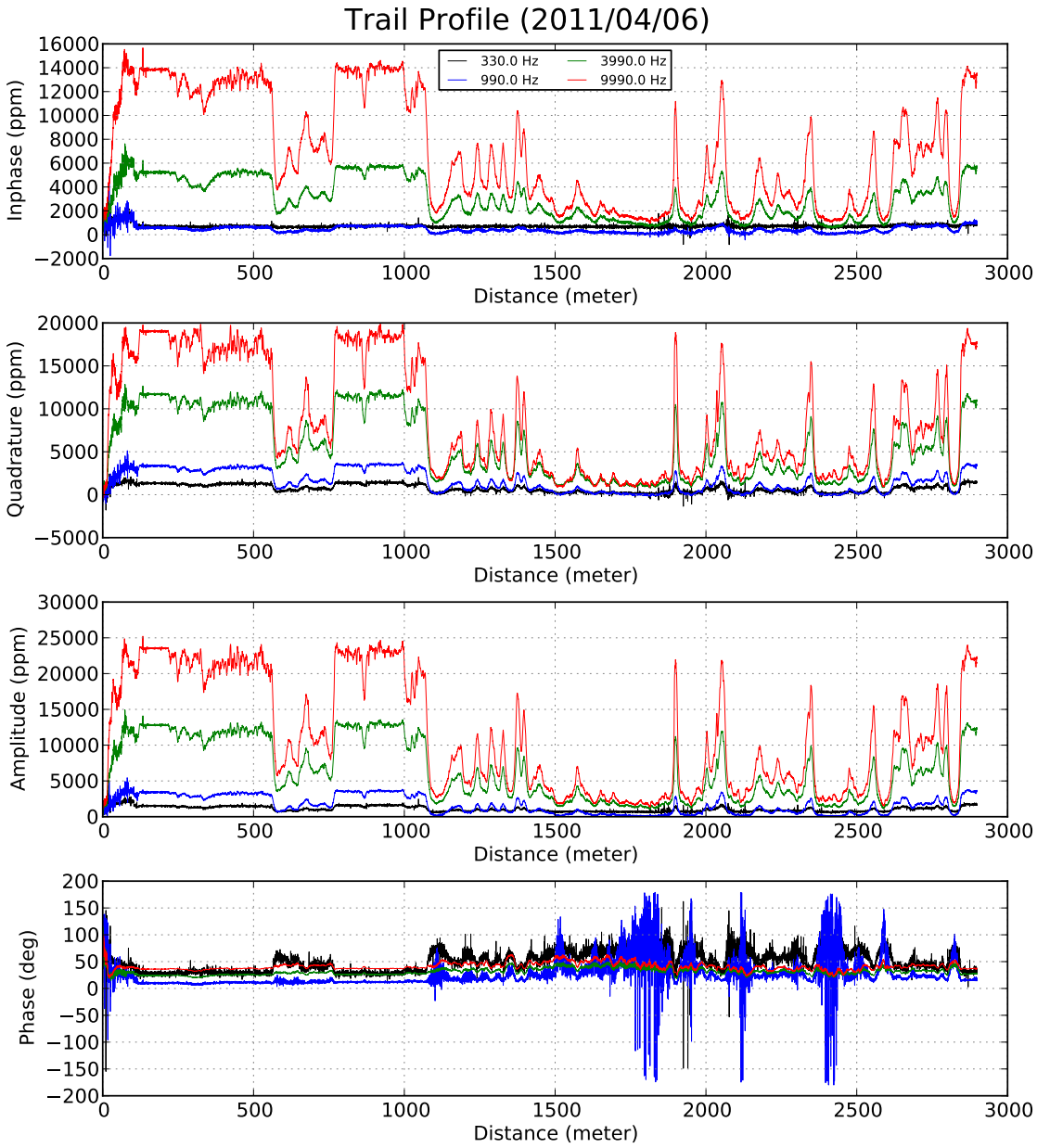

Figure 3.10.: Multi-frequency EM data of roughly 3 km long profile from the coast to the ridge location

3.2. Surface Nuclear Magnetic Resonance

Along the pressure ridge several surface nuclear magnetic resonance (SNMR) soundings were performed. SNMR measurements always incorporate a transmitter coil and a receiver coil of several meters in diameter, depending on the wanted sounding depth and expected amount of liquid water. Across the surveyed pressure ridge six so called coincident loop configurations, where the transmitter coil is also used as a receiver, and six separate coil configurations were used (see Figure 3.11). The combination of all 12 soundings provides a 2D coverage of the surveyed ridge allowing to invert for a distribution of liquid water across the ridge.
Every sounding consisted of a maximum of 32 pulse moments q, i.e. of 32 individual measurements. To increase the signal to noise level measurements for the same pulse moments are stacked. Only two stacks were needed here, since the noise level was mostly below 10 nV, which is extremely low compared to SNMR in regions with artificial noise created by e.g. power lines and railways. All coincident and separate loop soundings together consisted of $32 \times 2 \times 12 = 786$ measurements, which could be done during one day, including assembling and disassembling of the instrument.
The SNMR instrument itself was a NUMIS POLY of Iris Instruments which consists of two tuning capacitors, two DC/DC converters, four 12 V car batteries and the transmitter unit. All this could be mounted on a Nansen sledge from which the measurements were performed (see Figure 3.11). In addition a Laptop with the operating software was needed and 440 m of isolated copper cable to lay out the transmitter and receiver loops respectively. Each antenna loop was rectangular shaped with a side length of 20m × 20m and consisted of two turns in order to create a large enough dipole moment.

The raw data of every sounding were preprocessed already in the field in order to obtain sounding curves of imaginary and real part or amplitude and phase respectively (see Figure 3.12). Following the theory of SNMR as described in *Hertrich* (2008), the quantity which was obtained for every pulse moment q is the voltage V_0. The measured and fitted sounding curves for the coincident loop locations look promising, since they agree quite well with a 3D synthetic example which was calculated in beforehand the field campaign. However, the fitting curves which are shown in Figure 3.12 are preliminary. It is expected to find by using a suitable inversion scheme a subsurface model, i.e. a distribution of water and electrical conductivity, which describes the measured sounding curves better. This is exactly the challenge for the processing of the SNMR data sets and is scheduled for the next months.
In addition to the standard SNMR soundings so called T1 soundings were performed on positions L1 and L6. From T1 is used to infer information about the pore structure. Here we examine if this is also possible on sea ice. For the obtainment of T1 we followed a measurement scheme as proposed by *Walbrecker et al.* (2011). In hydrological targets T1 we used two sequential transmitter pulses instead of a single one, where the

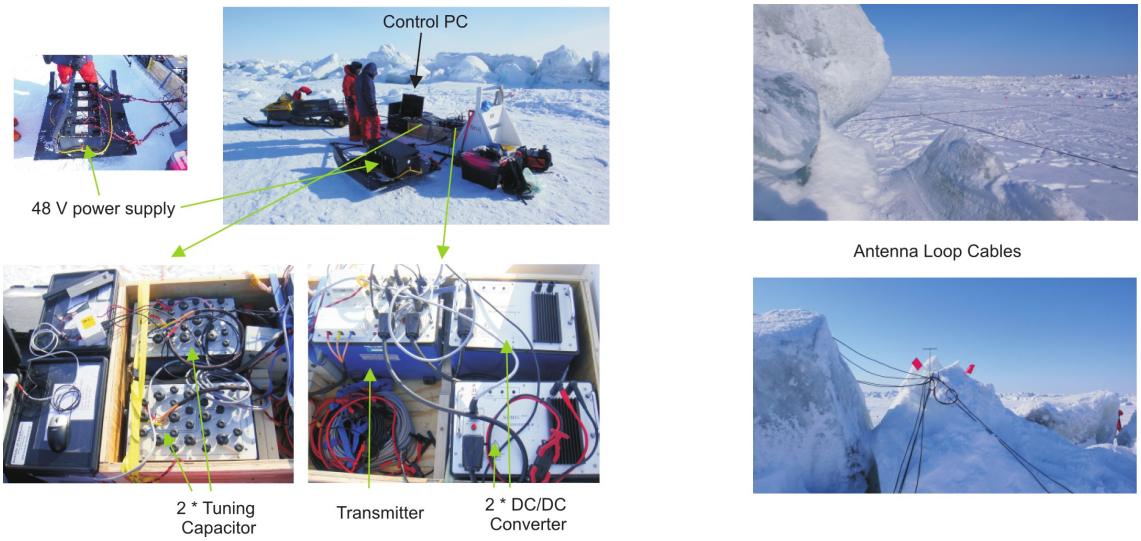

(a) Instrumentation and example of loop setup on deformed sea ice

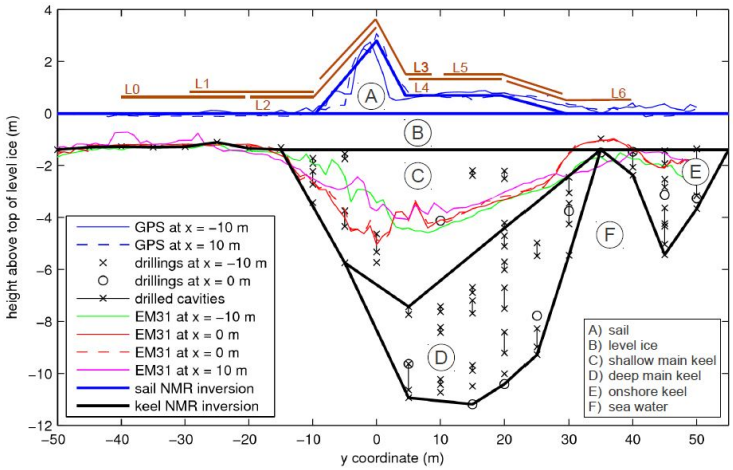

(b) Locations of transmitter and receiver loops (L0 - L6)

Figure 3.11.: Setup of SNMR measurements

second pulse is one time phase shifted by 90° and a second time in-phase with the first pulse. The delay between the first and second pulse was varied between 100 and 2900 ms. Processing of the T1 soundings is also scheduled for the next months.

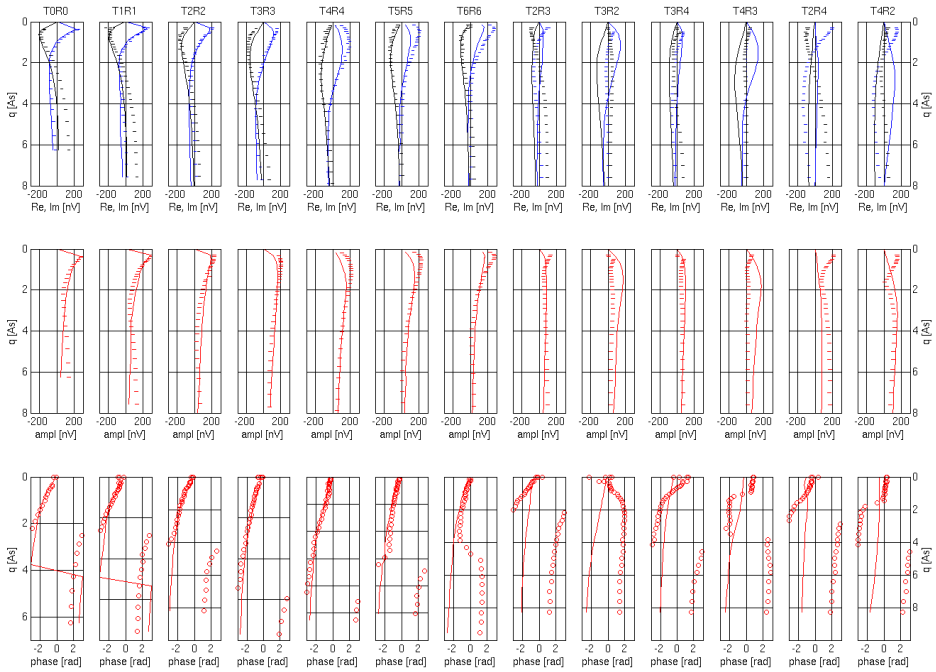

Figure 3.12.: Shown are the 13 soundings where T stands for transmitter and R for receiver and the number represent the location as shown in Figure 3.11. Measured values are shown as bars or circles and the solid lines are fitting curves derived from an estimated subsurface model. First row shows imaginary (black) and real (blue) part and the second and third rows amplitude and phase

3.3. Electrical Resitivity Tomography

A multi electrode DC-Geoelectric instrument ("GeoTom RES/IP") was used in order to obtain the distribution of electrical resistivity within the pressure ridge. Such measurements are referred to as electrical resistivity tomography (ERT). The main motivation for the ERT measurement was to obtain and use a most realistic conductivity distribution model for the electromagnetic forward modeling involved in the inversion of surface NMR data. But even a solitary ERT measurement across the ridge is of interest, since electrical conductivity is already an indirect indicator for the amount of sea water within the pressure ridge volume. One line of 75 m length with an electrode spacing of 0.5 m was measured across the ridge starting at coordinate (0,-25) and ending at coordinate (0,50) (see Figure 3.1). The following parameters were chosen for the ERT measurements:

- number of electrode positions: 150 (100 for one run)
- Configuration: Wenner, down to 24 levels
- Electrode spacing: 0.5 m
- Frequency: 4.16 Hz
- Maximum current strength: 5 mA

The electrodes consisted of 30 cm t-shaped stainless steel metal spikes with a hole of 0.5 cm in diameter at the top to connect banana plug cables (see Figure 3.13). To guarantee the best possible electrical coupling to the sea ice, the electrodes were pressed approximately 5 cm deep into 1 cm diameter drill holes. Before the start of the actual measurements every electrode was sprinkled with sea water. Four electrode cables, each 50 m long and with 25 channels, connected the electrodes to the 100 channel GeoTom RES/IP instrument. In total two Wenner measurements involving all 100 electrodes were needed to complete the entire 75 m long transect. The first measurement incorporated electrodes between coordinates (0/-25) and (0/25) and the second measurement electrodes between coordinates (0/0) and (0/50), each measurement took about 4 hours. This was longer than expected due to bad coupling of several electrodes. For each of the two Wenner measurements the electrode coupling to the ice was tested by resistivity measurements between two adjacent current electrodes. In most cases the coupling resistivity was below 10 ohmm, but for a couple of electrodes on the ridge, especially close to the sail, the coupling was sometimes as bad as 3000 ohmm. Badly coupled electrodes are isolated from the injected current system and are therefore excluded for the inversion of the ERT data. The two pseudo sections including all measured electrode combinations are shown in Figure 3.14. Below depth level 10 the measured resistivity values were not very reliable any longer, which can be seen

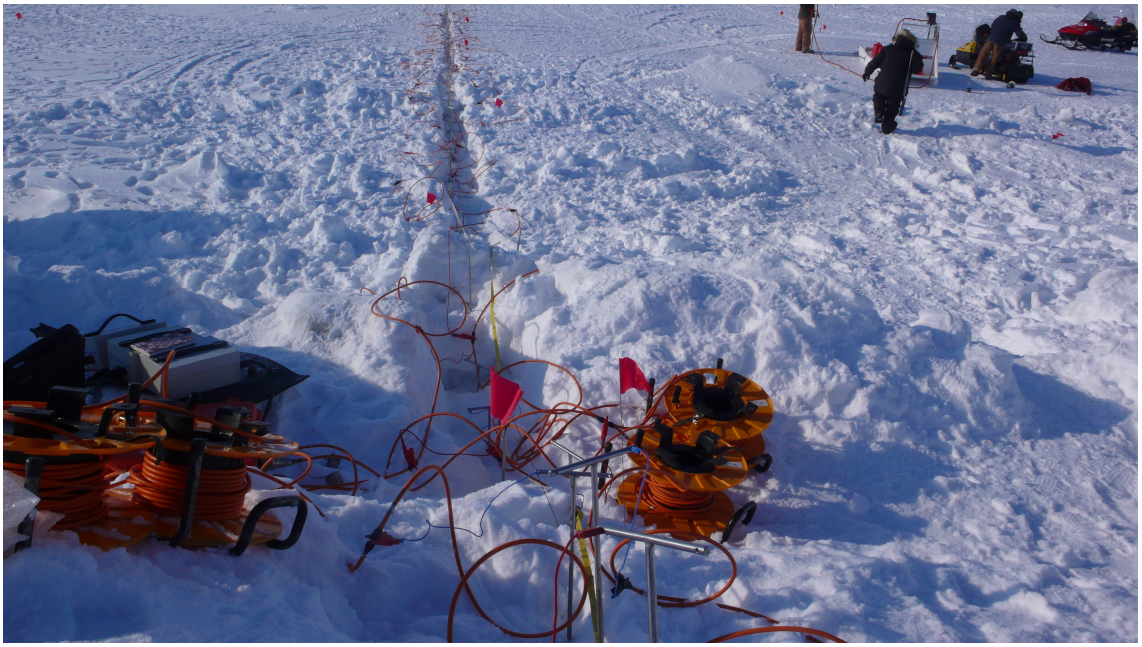

Figure 3.13.: Photo of ERT setup. Shown are the electrodes between $y = -25$m and $y = 0$m

by stripe liked features in the pseudo sections. These stripes are an indicator that bad ice coupling of a single electrode starts to dominate the measurement which no longer contains information from deeper regions.
After both Wenner measurements were merged together and the topography of the DGPS measurements was included, the first 10 levels of the complete transect were inverted into a resistivity depth section. The used 2D inversion program "DC2DInvRes" (http:dc2dinvres.resistivity.net) was provided by Thomas Günther from the Leibnitz Institute of Geophysics, Hannover. For the inversion all those measurement values with apparent resistivities higher than 1000 Ohmm were neglected. The resulting depth section is shown in Figure 3.15. Clearly visible are the low resistivity values of the open water zones and the higher resistivity values where consolidated ice is present. Due to the strong anisotropic behavior of the electrical conductivity of sea ice, which is not accounted for in the inversion program, the thickness of level ice is underestimated in the resistivity section. The inversion of the first 10 levels provides information down to the first 5 m, which is unfortunately shallower than the ridge (see Figure 3.8). Interestingly, already the ERT section shows zones of high conductivity within the ridge, which may refer to liquid water.

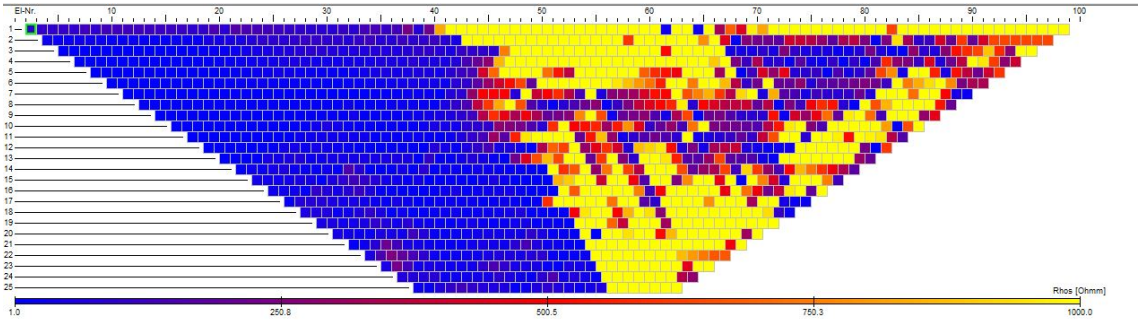

(a) $y = -25\text{m} - y = 25\text{m}$

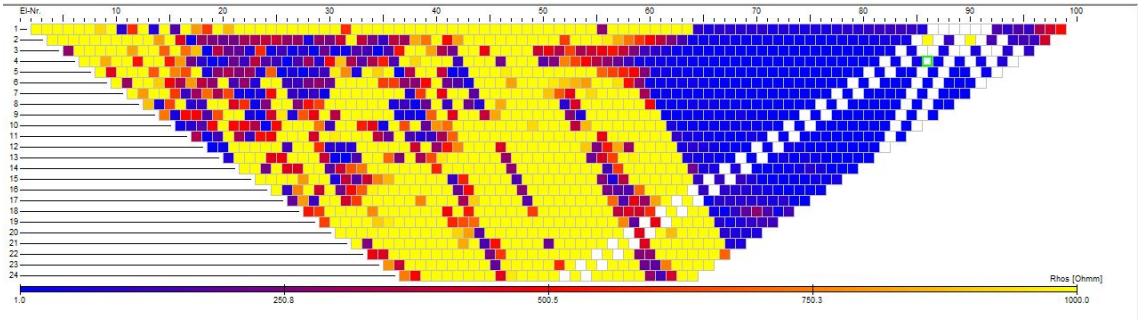

(b) $y = 0\text{m} - y = 50\text{m}$

Figure 3.14.: Resistivity of pressure ridge from pseudo sections of two ERT Wenner configurations

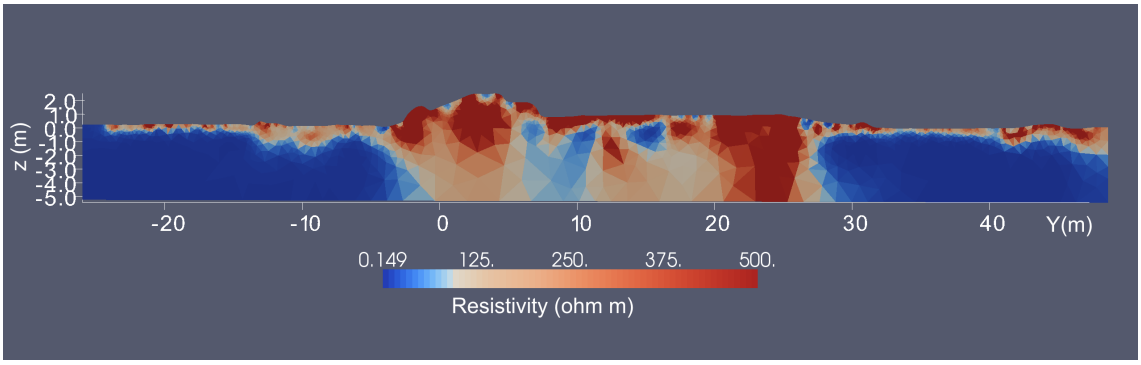

Figure 3.15.: Resistivity depth section of ERT data from 2D inversion

4. Deliverables

4.1. List of HEM Profiles

`HEM_PAM11_20110331T002823_20110331T021537`

Date : 2011/03/30

Survey with Polar-5 west of Barrow. The flight route was chosen to survey sites of several moorings as well as Hanna Shoal. Problems with statics caused by icy fog lead to sporadic disruptions of the Bird operation.

`HEM_PAM11_20110402T231131_20110403T003931`

Date : 2011/04/02

Survey with Polar-5 north-east of Barrow towards a band of multi-year ice.

Table 4.1.: List of Profiles

4.2. File Naming Conventions

The filename contains a shortcut for the campaign and the start and stop time of the data file. The id for the SIZONet 2011 field campaign is given by `PAM11` (as part of the PAM-ARCMiP project).

`HEM_CMPID_SSSSSSSSSSSSSS_PPPPPPPPPPPPPP.dat`

Token	*Description*
`CMPID`	Contains campaign name (3 letters + 2 digits of year)
`SSSSSSSSSSSSSS`	`YYYYMMDDTHHMMSS` : Start and Stop time
`PPPPPPPPPPPPPP`	

Table 4.2.: File naming convention of EM data files

4.3. Data Format

The EM data is delivered in blank separated ASCII data format described in table 4.3. All time tags are standard UTC time.

Column	*Description*	*Format*	*Unit*
1	Year	I4	–
2	Month	I2	–
3	Day	I2	–
4	Time	F8.2	Seconds of the day
5	Fiducial Number	I9	–
6	Latitude	F12.7	degree
7	Longitude	F12.7	degree
8	Distance	F12.3	m
9	Thickness	F8.3	m
10	Laser Range	F8.3	m

Table 4.3.: File format for EM data delivery

One flight is separated into several profiles with a calibration at the beginning and the end. The distance flown is calculated for this individual profiles and therefore not cumulative for the entire flight. The fiducial number can be discontinuous if a reboot of the system was necessary during the flight.

A. GEM-2 Calibration

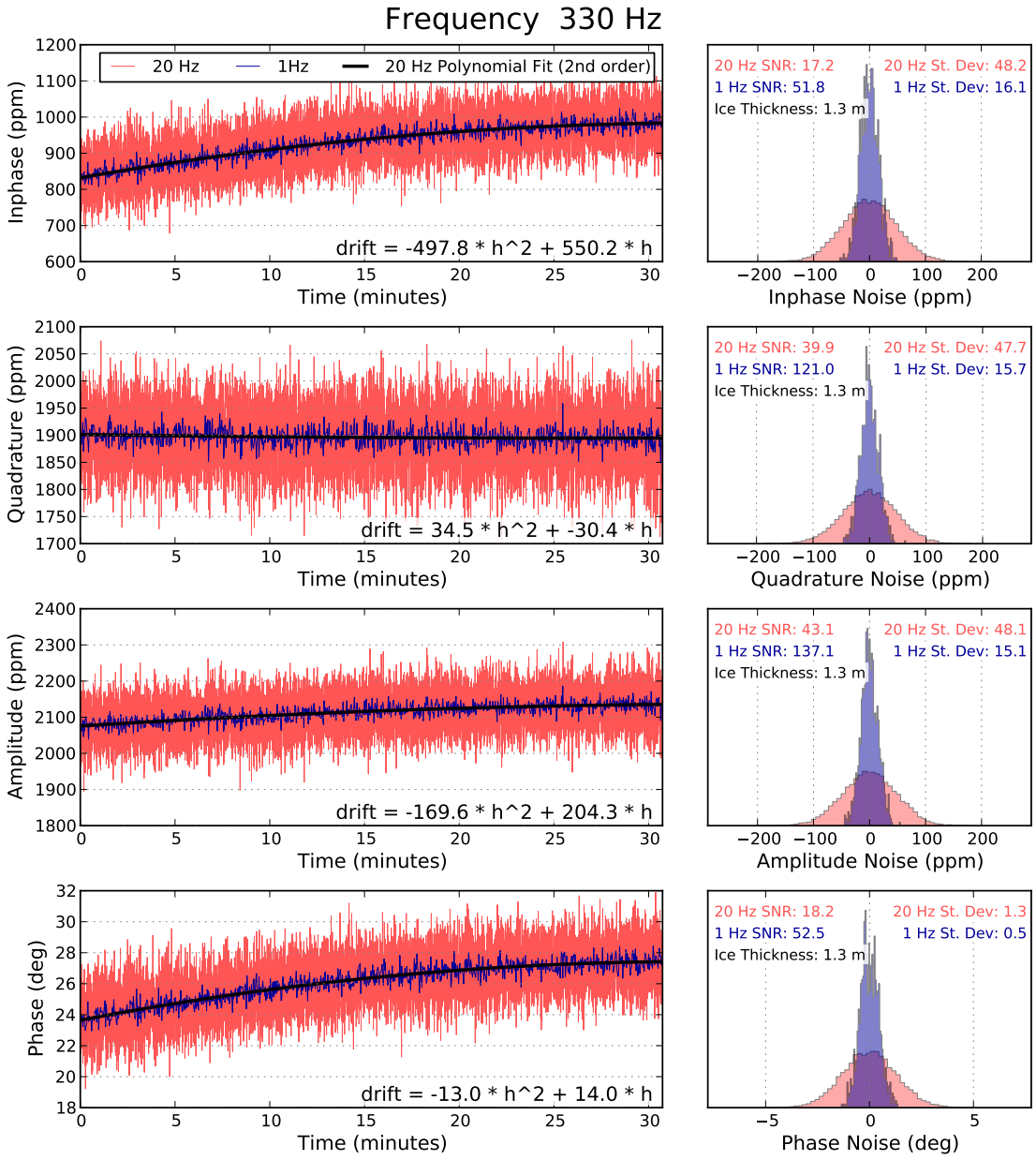

Figure A.1.: Drift and Noise of measured EM parameters at 330 Hz

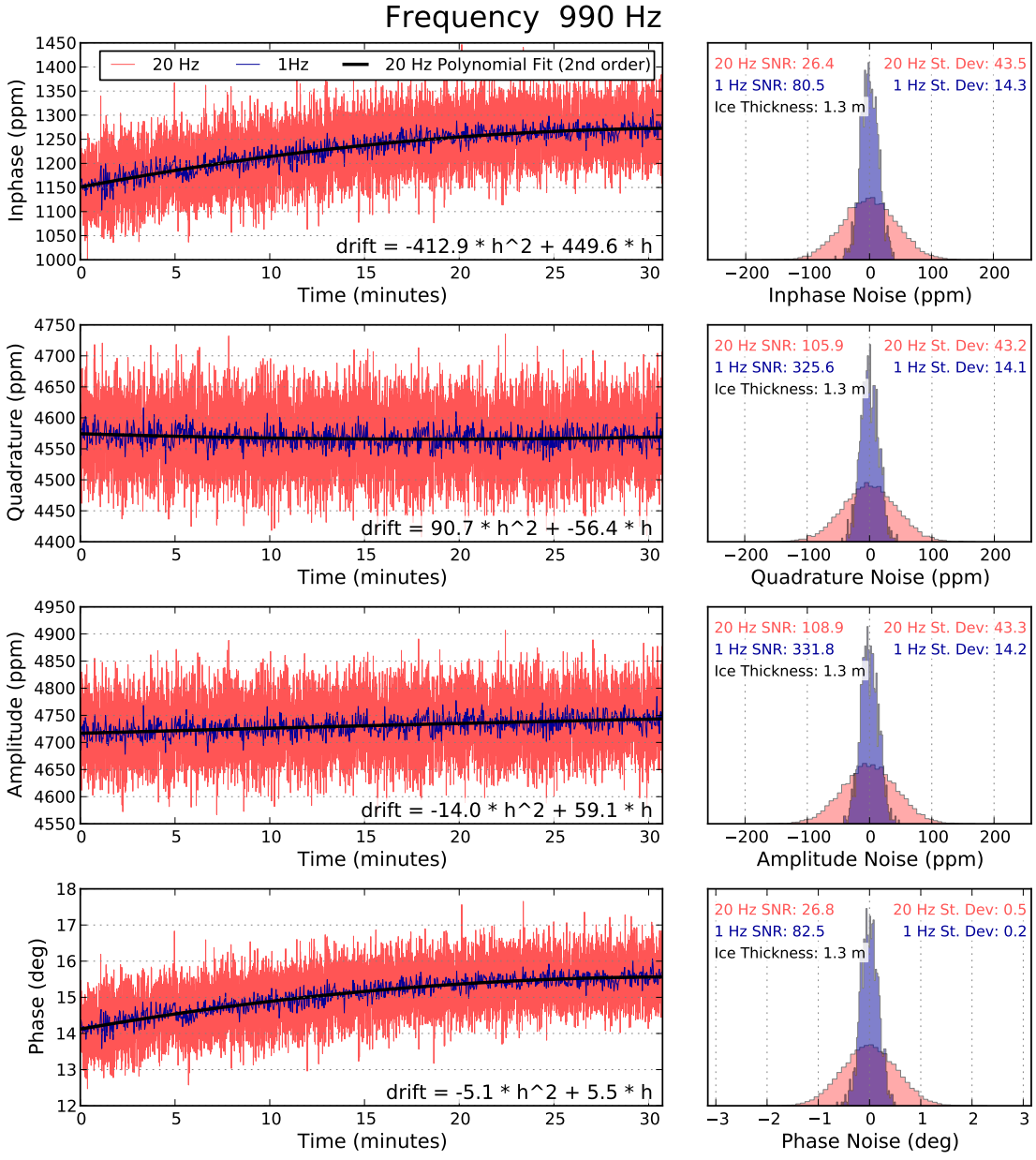

Figure A.2.: Drift and Noise of measured EM parameters at 990 Hz

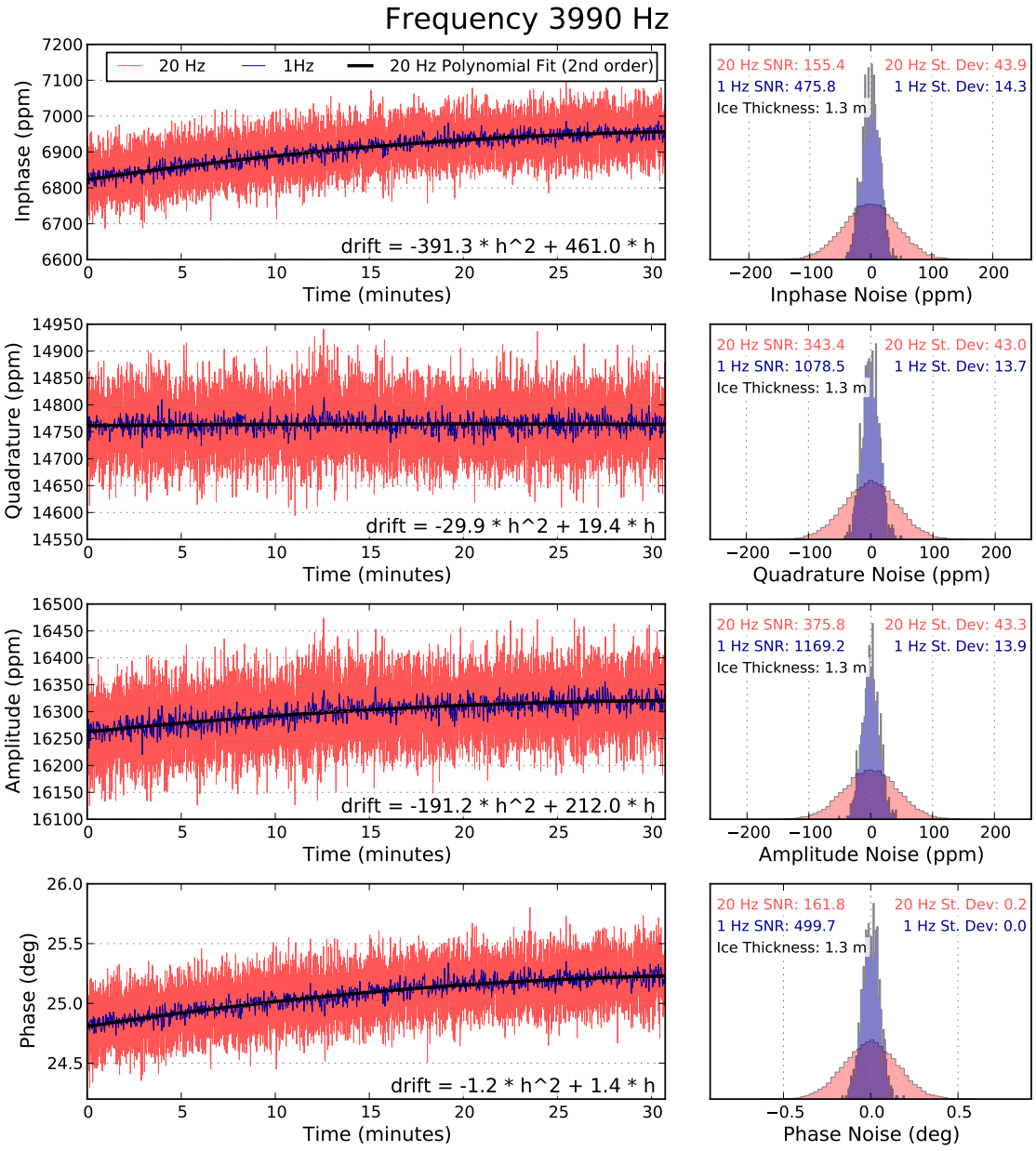

Figure A.3.: Drift and Noise of measured EM parameters at 3990 Hz

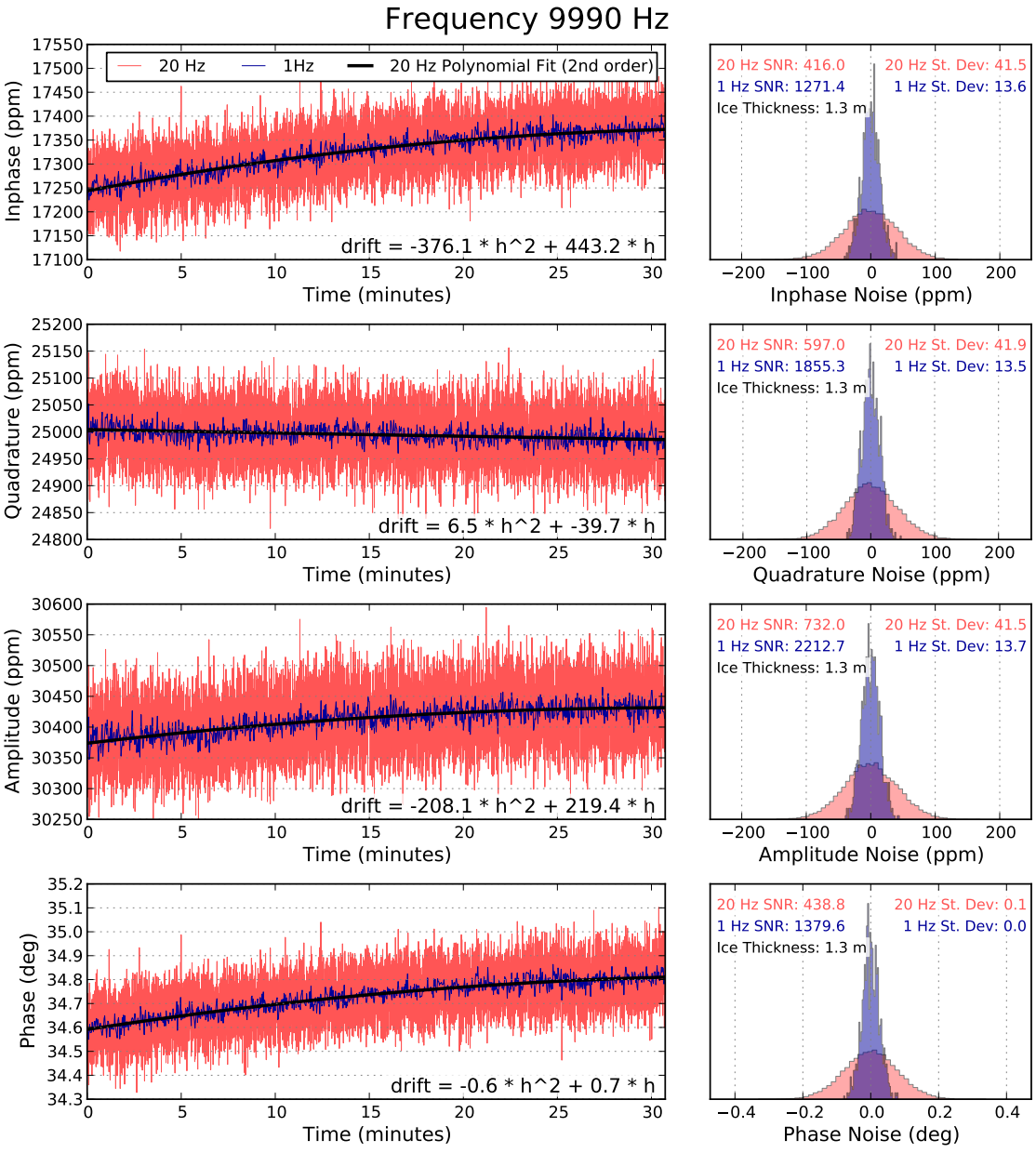

Figure A.4.: Drift and Noise of measured EM parameters at 9990 Hz

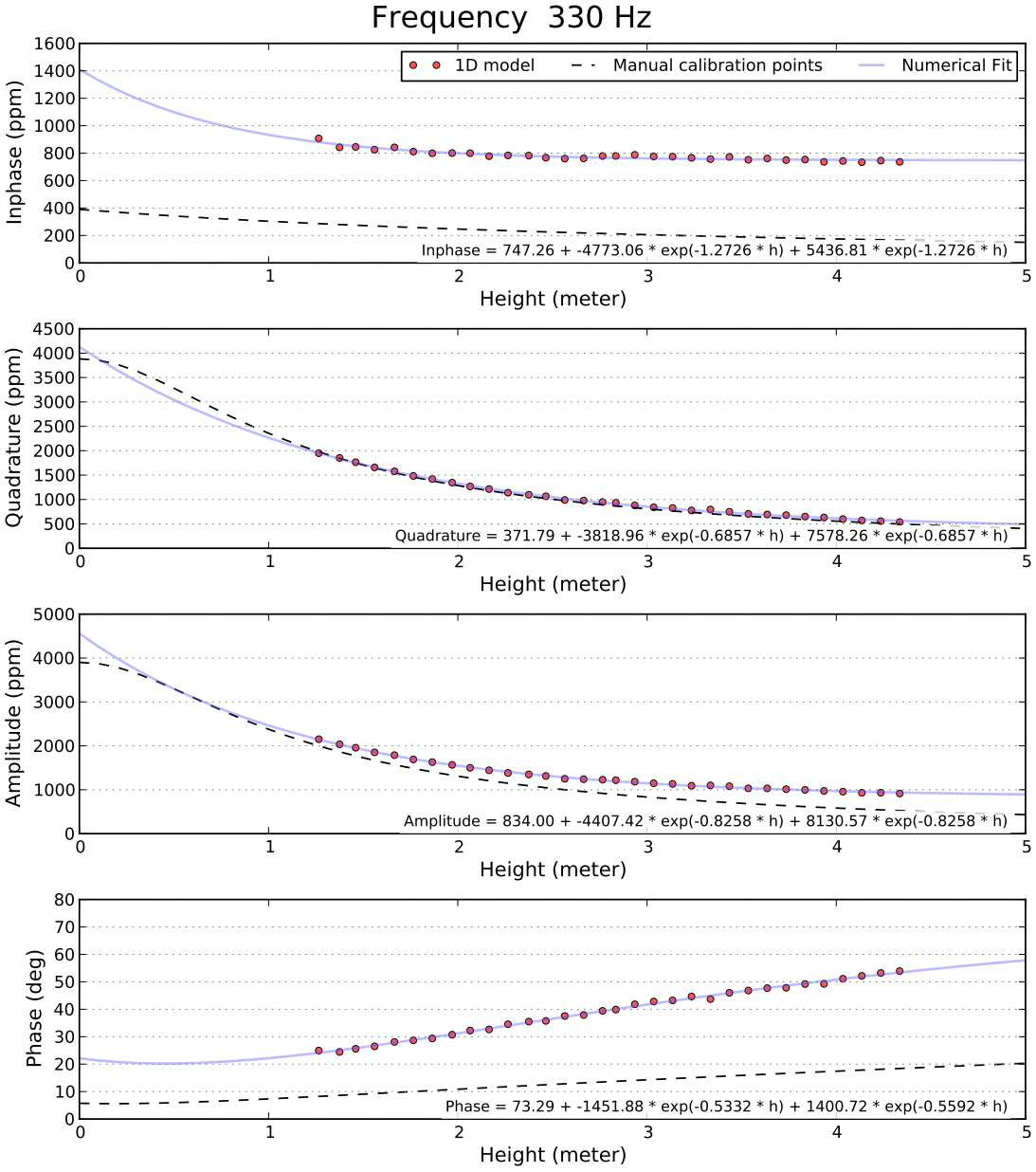

Figure A.5.: Comparison of measured EM parameters and 1D forward model at 330 Hz

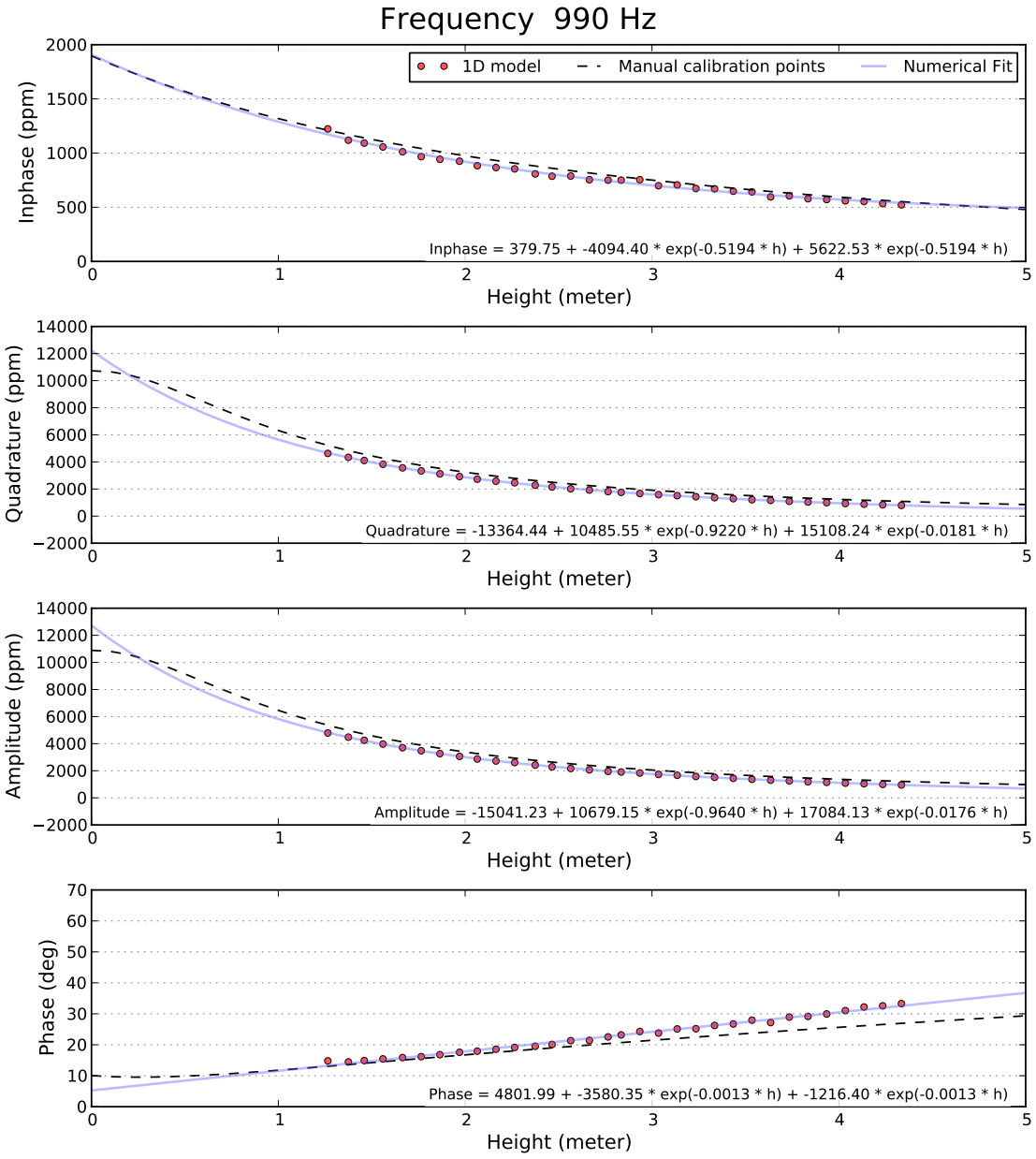

Figure A.6.: Comparison of measured EM parameters and 1D forward model at 990 Hz

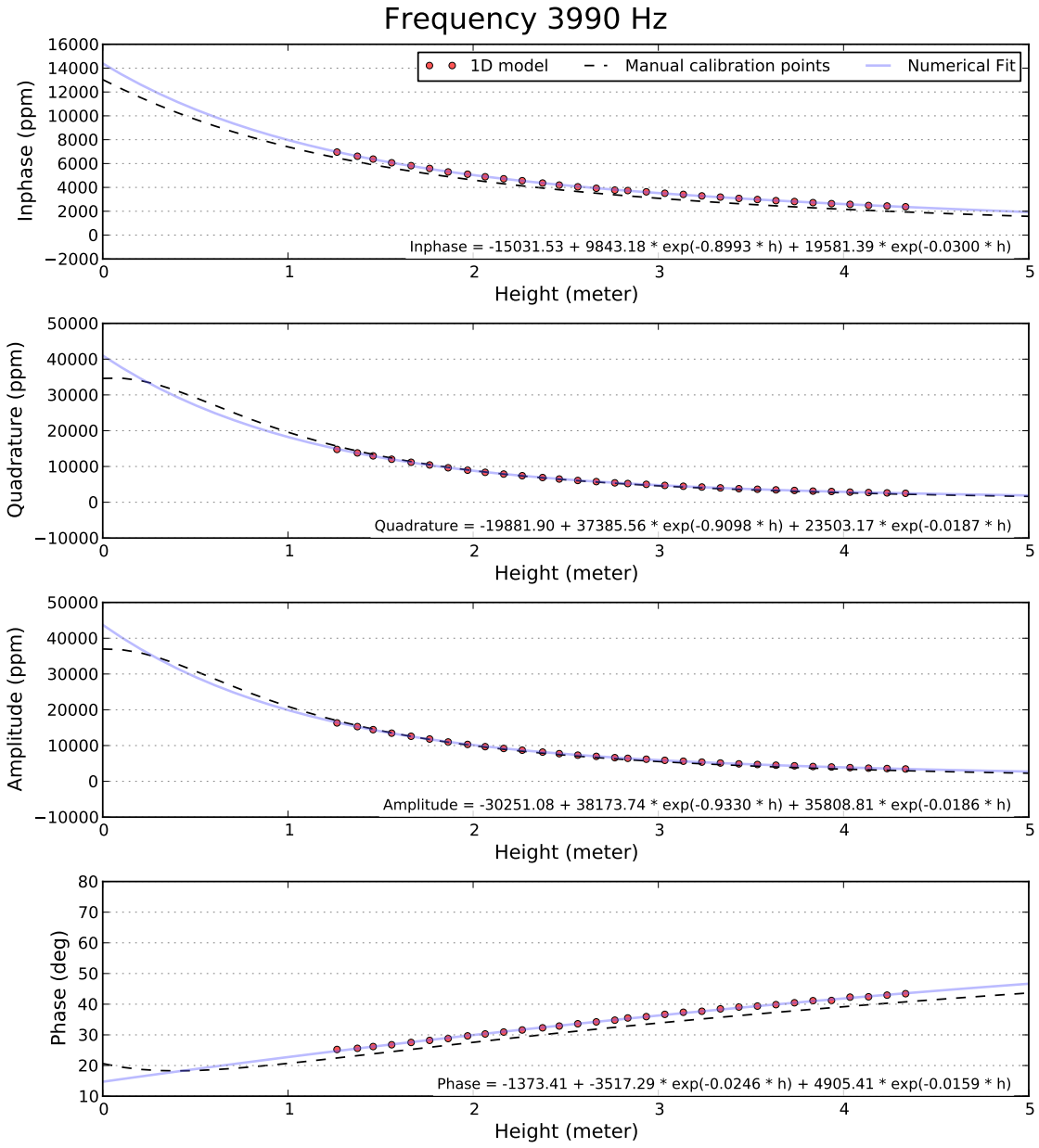

Figure A.7.: Comparison of measured EM parameters and 1D forward model at 3990 Hz

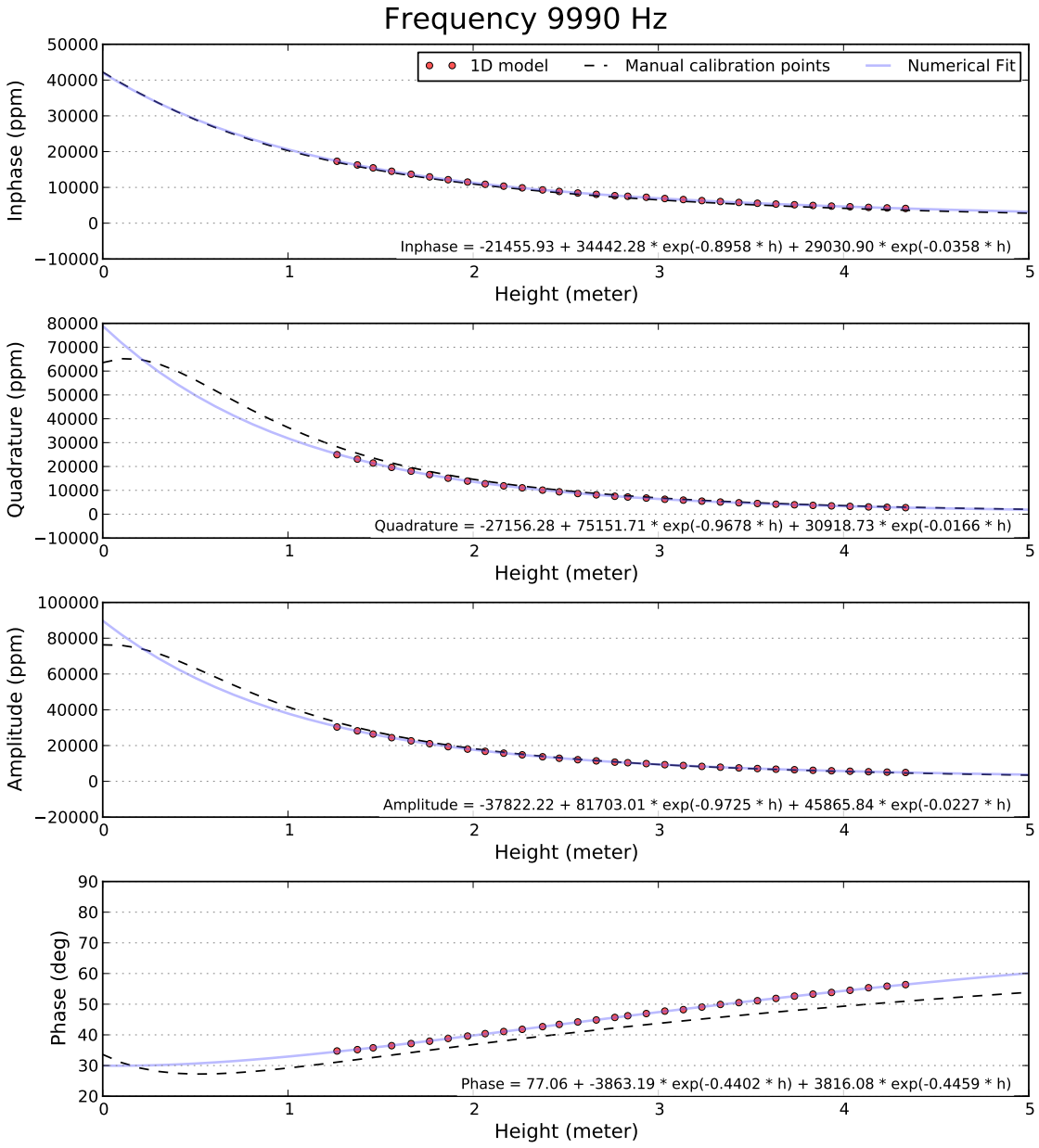

Figure A.8.: Comparison of measured EM parameters and 1D forward model at 9990 Hz

List of Figures

2.1. Polar-5 in Barrow during SIZONet 2011. The EM-Bird can be seen below the aircraft body. 2
2.2. EM-Bird in operational mode on Polar-5. The 200 ft tow cable provides power to the instrument. Real-time data transfer is realized by a wireless network. 4
2.3. Mean sea ice thickness averaged over 5 km sections for two flights during the SIZONet 2011 field experiment. 2011/03/30: West of Barrow, 2011/04/04 North-east of Barrow 5
2.4. Sea ice thickness histograms from both Polar-5 surveys 6
2.5. Sea ice thickness from two overflights (perpendicular crossings) over Hanna Shoal. (FID: record number) 6
2.6. Map of photo locations along survey over fast ice zone. The red dot marks the site of the EM multi-sensor study (not covered by any image) 7
2.7. Example of image composite over Barrow landfast sea ice at the location of a whaling trail 8

3.1. Layout of measurements of a multi-sensor study of a pressure ridge in landfast sea ice. Three lines with an individual length of 100 m and a spacing of 20 meters were used to align data collected from EM sensors and drilling 10
3.2. Horizontal coplanar (HCP) multi-frequency EM data of ridge at line x = 0 . 12
3.3. Vertical coplanar (VCP) multi-frequency EM data of ridge at line x = 0 . . . 13
3.4. Horizontal coplanar (HCP) multi-frequency EM data of ridge at line x = 10 14
3.5. Vertical coplanar (VCP) multi-frequency EM data of ridge at line x = 10 . . 15
3.6. Horizontal coplanar (HCP) multi-frequency EM data of ridge at line x = -10 16
3.7. Vertical coplanar (VCP) multi-frequency EM data of ridge at line x = -10 . . 17
3.8. Sea ice thickness obtained from the EM31 and steam drilling together with the locations of voids in the ridge 18
3.9. Location of trail surveyed with GEM-2. (Color: Inphase 9.99 kHz) 18
3.10. Multi-frequency EM data of roughly 3 km long profile from the coast to the ridge location 19
3.11. Setup of SNMR measurements 21

3.12. Shown are the 13 soundings where T stands for transmitter and R for receiver and the number represent the location as shown in Figure 3.11. Measured values are shown as bars or circles and the solid lines are fitting curves derived from an estimated subsurface model. First row shows imaginary (black) and real (blue) part and the second and third rows amplitude and phase 22
3.13. Photo of ERT setup. Shown are the electrodes between $y = -25$m and $y = 0$m 24
3.14. Resistivity of pressure ridge from pseudo sections of two ERT Wenner configurations 25
3.15. Resistivity depth section of ERT data from 2D inversion 25

A.1. Drift and Noise of measured EM parameters at 330 Hz 29
A.2. Drift and Noise of measured EM parameters at 990 Hz 30
A.3. Drift and Noise of measured EM parameters at 3990 Hz 31
A.4. Drift and Noise of measured EM parameters at 9990 Hz 32
A.5. Comparison of measured EM parameters and 1D forward model at 330 Hz 33
A.6. Comparison of measured EM parameters and 1D forward model at 990 Hz 34
A.7. Comparison of measured EM parameters and 1D forward model at 3990 Hz 35
A.8. Comparison of measured EM parameters and 1D forward model at 9990 Hz 36

List of Tables

4.1. List of Profiles 26
4.2. File naming convention of EM data files 27
4.3. File format for EM data delivery 27

Bibliography

Hertrich, M., Surface Nuclear Magnetic Resonance Tomography, *Progress in Nuclear Magnetic Resonance Spectroscopy, 53,* (4), 227–248, 2008.

Walbrecker, J. O., M. Hertrich, J. A. Lehmann-Horn und A. Green, Estimating the longitudinal relaxation time T(1) in surface NMR, *Geophysics, 76,* (2), F111–F122, 2011.